NC STATE UNIVERSITY

EIC Theory Overview

Andrey Tarasov

GHP 2025, March 14, 2025

The fundamental structure of visible matter

- Hadron is characterized by complex dynamics of parton interactions
- Due to running of the coupling constant one has to understand the hadron as a many-body parton system which is strongly bounded - dense QCD medium
- How protons and neutrons emerge from their basic quark and gluon constituents?

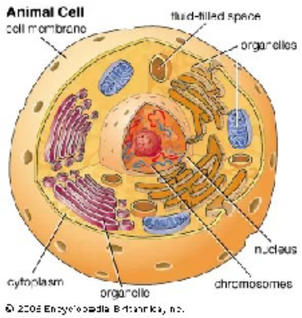

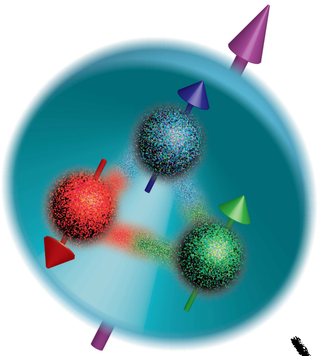

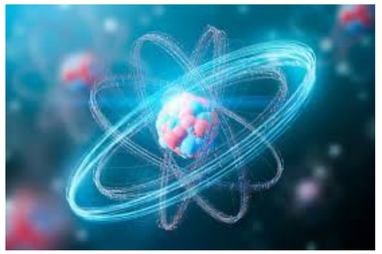

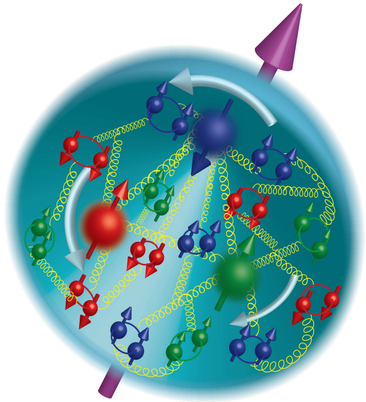

Quarks and gluons: understanding the strong nuclear force

EIC will be instrumental in understanding “how the characteristic properties of the proton, such as mass and spin, arise from the interactions between quarks and gluons, and how new phenomena and properties emerge in extremely dense gluonic, nuclear environments.”

The 2023 Long Range Plan for Nuclear Science

- How does the mass of the nucleon arise?
- How does the spin of the nucleon arise?
- What are the emergent properties of dense systems of gluons?

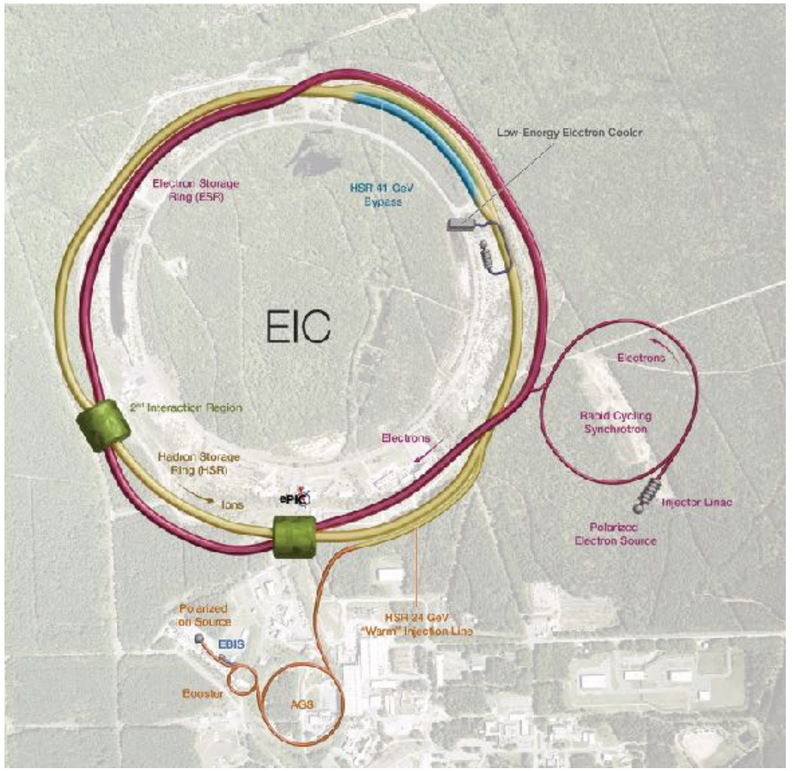

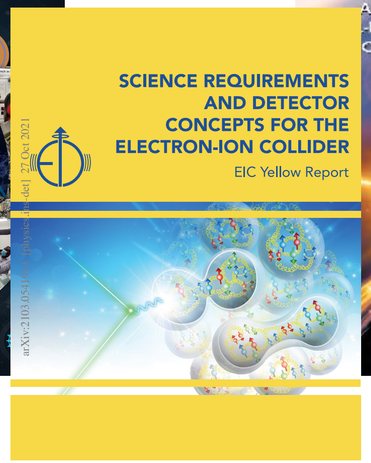

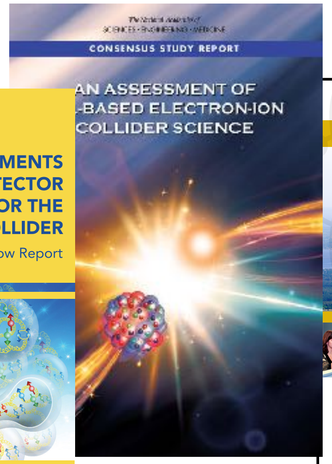

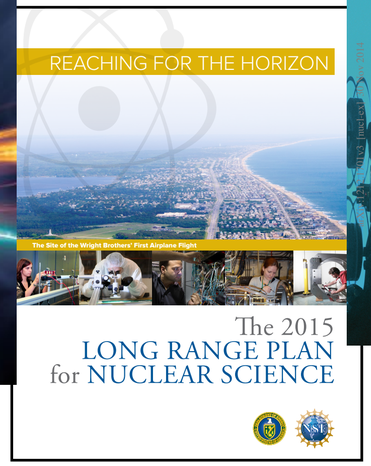

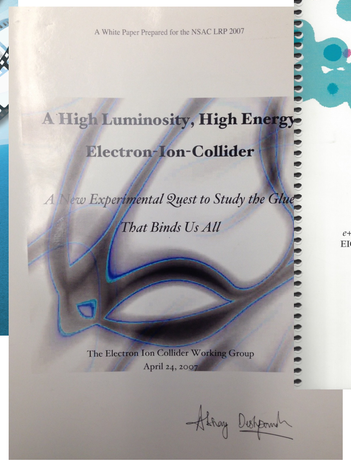

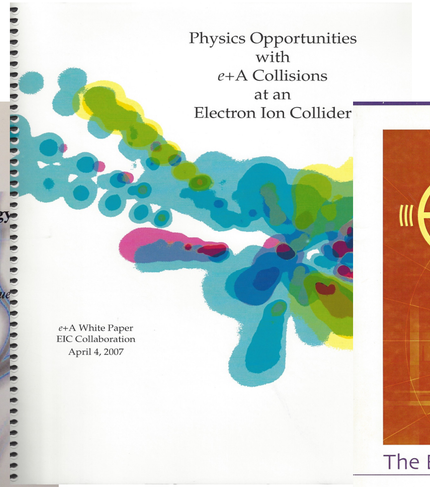

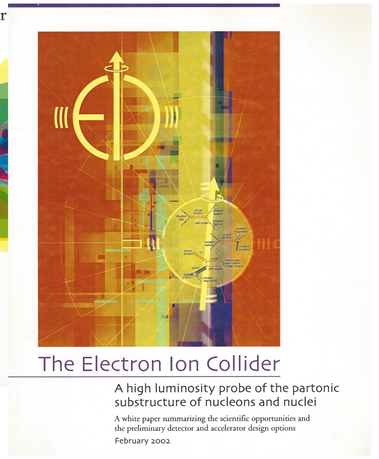

EIC Theory

Major physic goals:

- Understanding the properties of hadrons: proton mass and spin
- Precision imaging of hadrons: PDFs, TMDs, GPDs
- Saturation, properties of QCD at high parton density
- Jets
- Hadronization, initial geometry and fluctuation

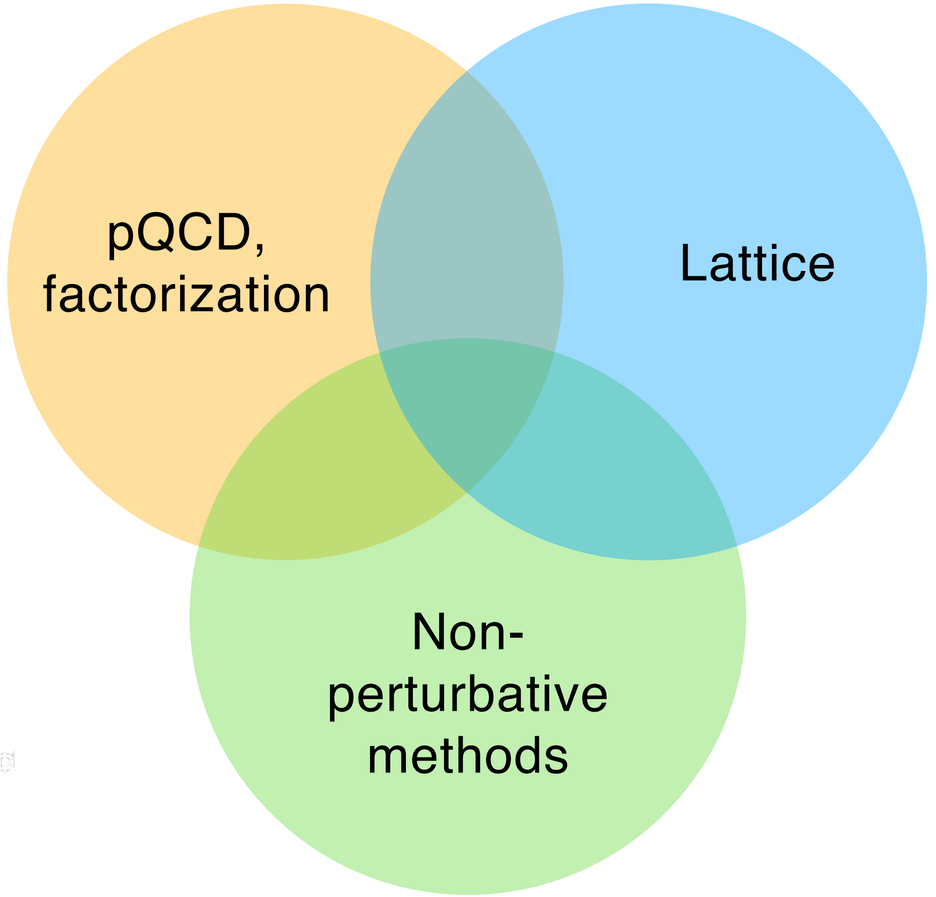

The electron beam is well under control!

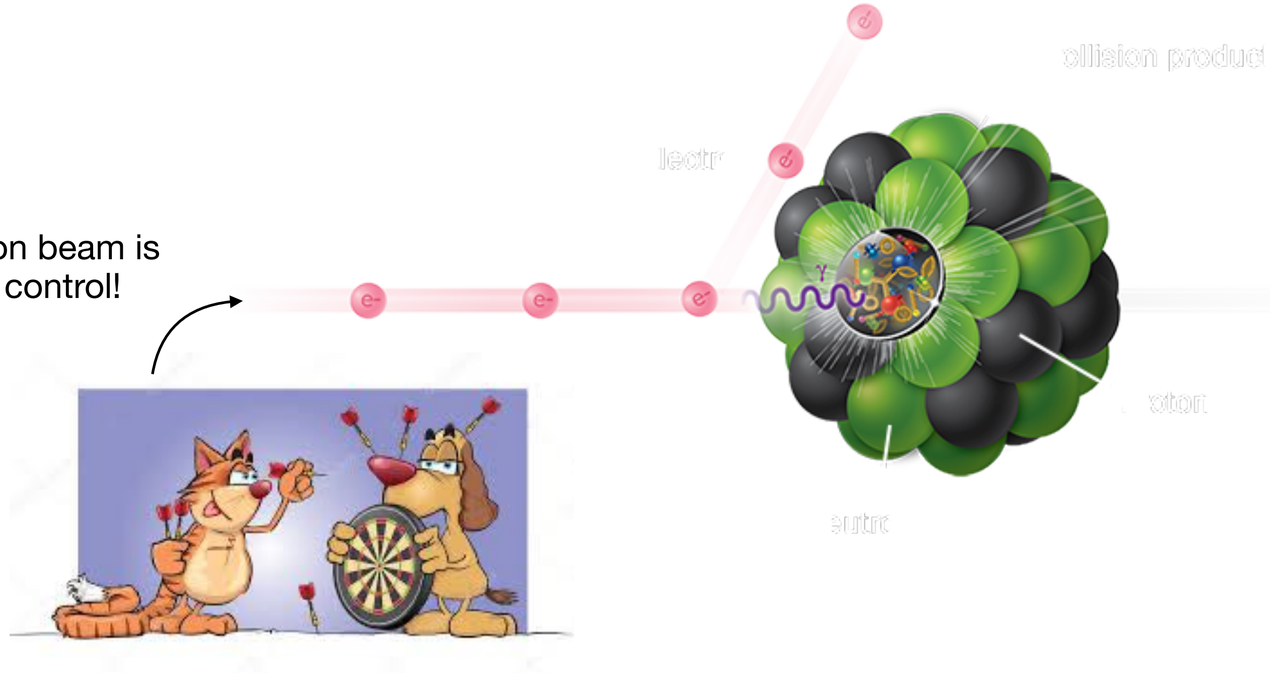

QCD Factorization

Hadron as a many body parton system. We cannot distinguish individual quarks and gluons!

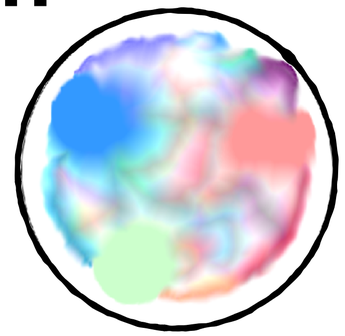

proton mass $\sim \Lambda_{QCD}$

size of proton $\sim \Lambda_{QCD}^{-1}$

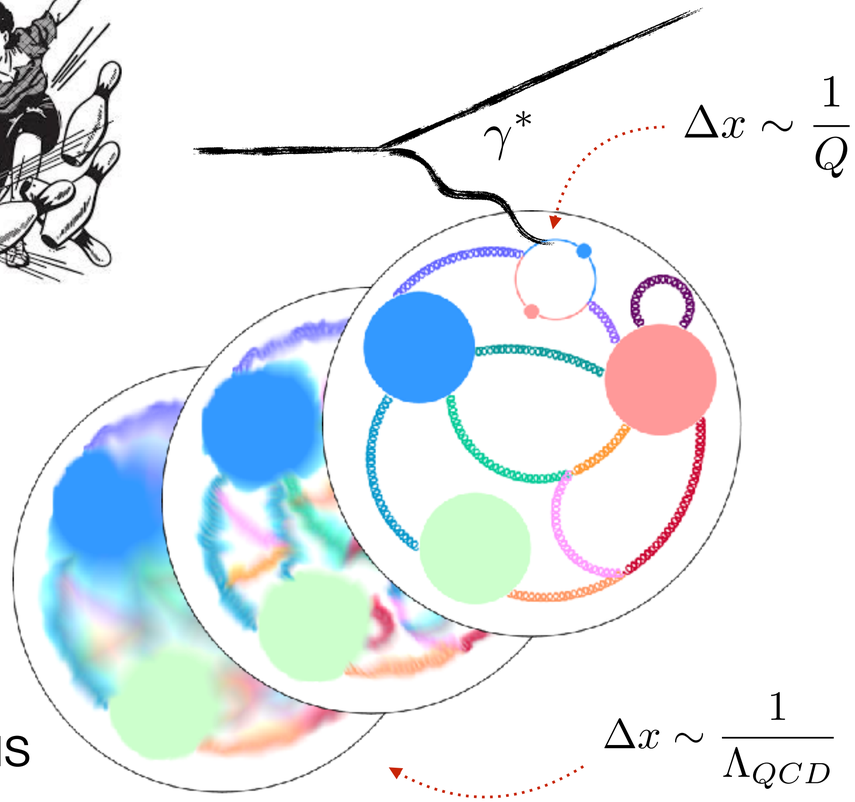

Interacting with external probe the hadron reveals different types of parton dynamics (large separation of scales!) → strong correlation between modes

$$W^{\mu\nu}(p,q) = \sum_f \int \frac{dx}{x} \mathcal{H}_f^{\mu\nu}(\tilde{k},q,\mu^2)\varphi_f(x,\mu^2) + \mathcal{O}(\Lambda^2/Q^2)$$

collinear factorization in DIS

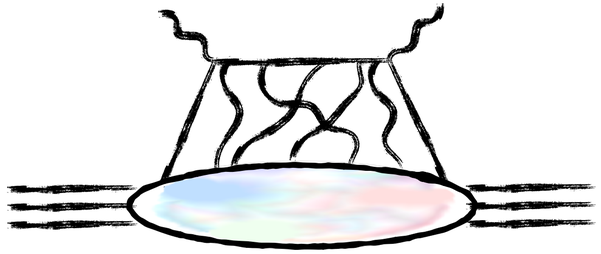

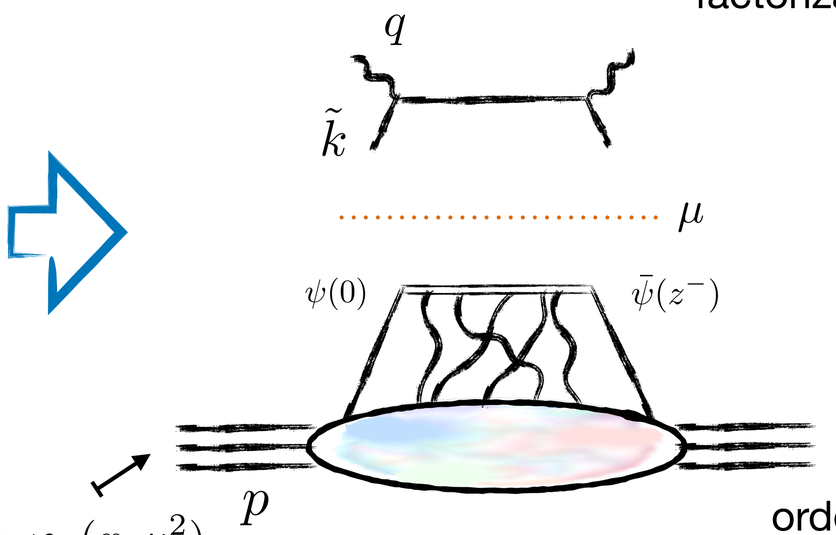

$$\int \frac{dz^-}{2\pi} e^{-ixp^+z^-} \langle P|\mathcal{O}_f(z^-)|P\rangle_{\mu^2} = \varphi_f(x,\mu^2)$$

$p_\perp \gg \mu$

$p_\perp \ll \mu$

ordering of the emission in transverse momentum

The non-perturbative mode can be written formally as a matrix elements of QCD operators → distribution functions to be extracted at EIC

One-dimensional picture (collinear PDFs)

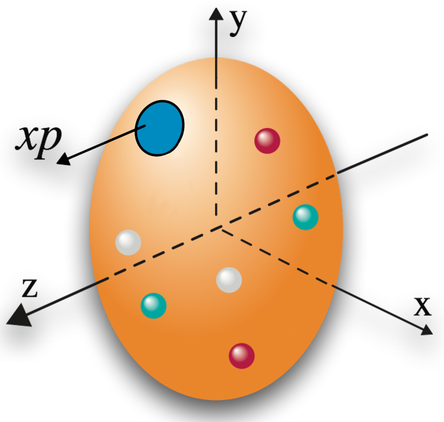

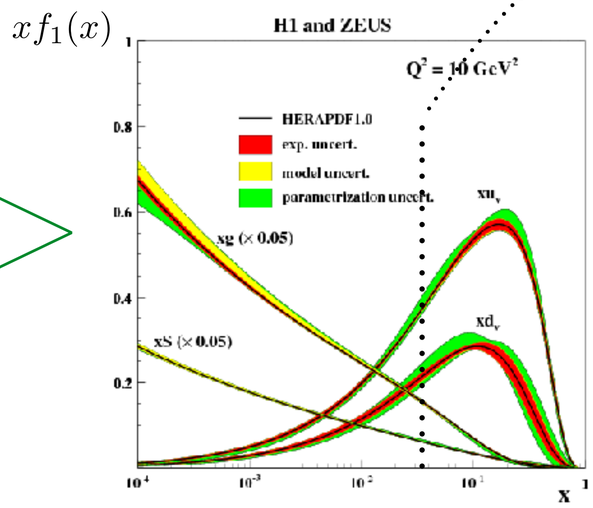

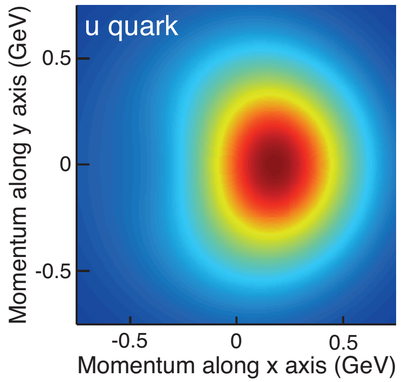

Three-dimensional picture (transverse momentum dependent distributions)

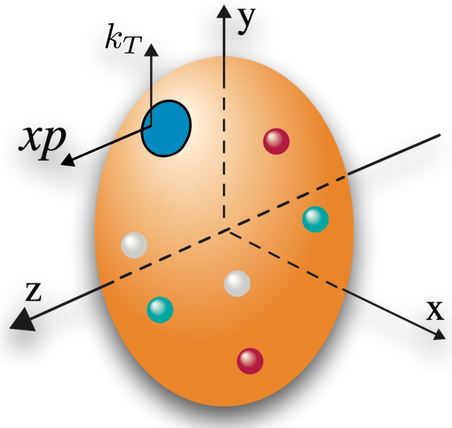

Each QCD factorization scheme defines it own set of distribution functions. Together these functions provide a detailed mapping of the structure of the dense QCD medium

Precision QCD tomography at EIC

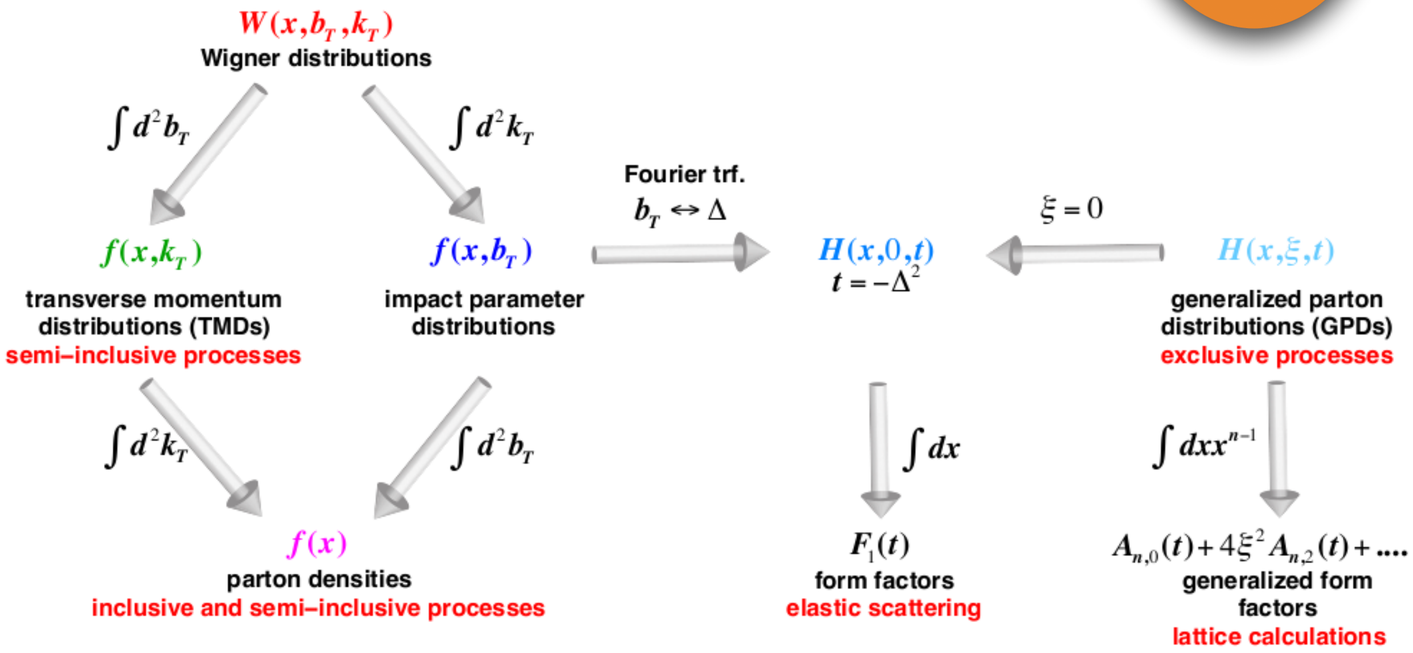

Extraction of PDFs: EIC impact

E. Aschenauer, R. Sassot and M. Stratmann,
Phys. Rev. D92 (2015) 094030

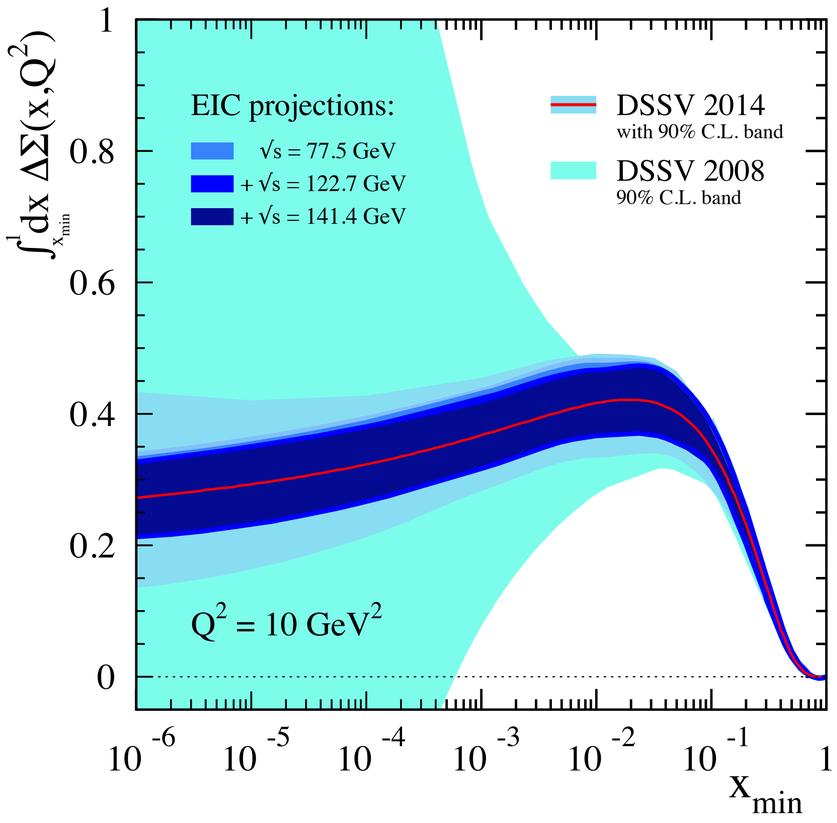

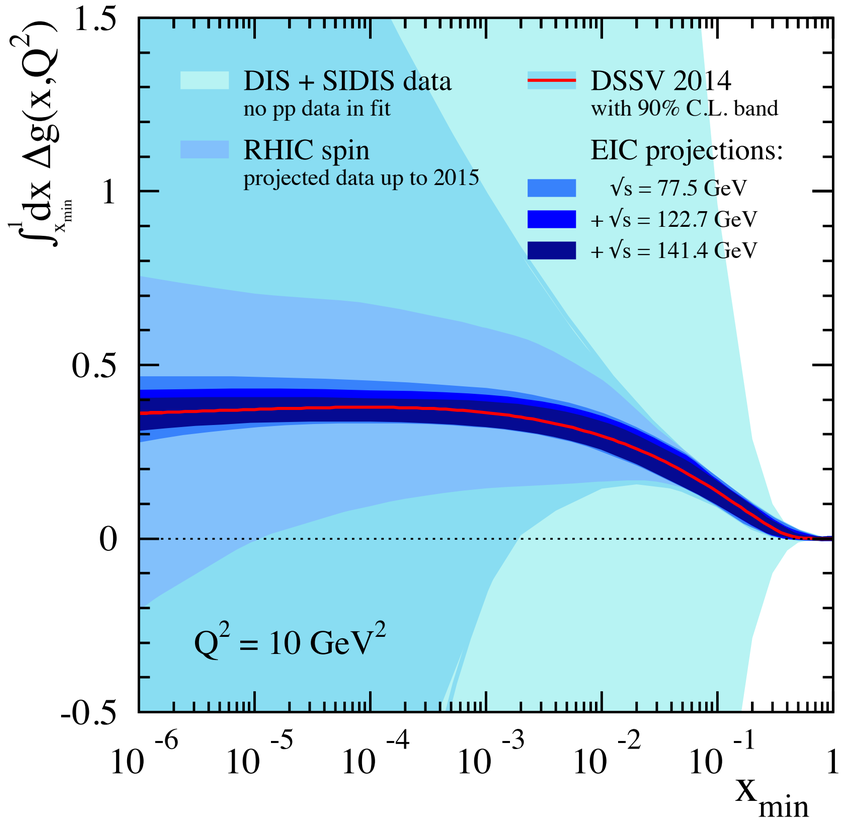

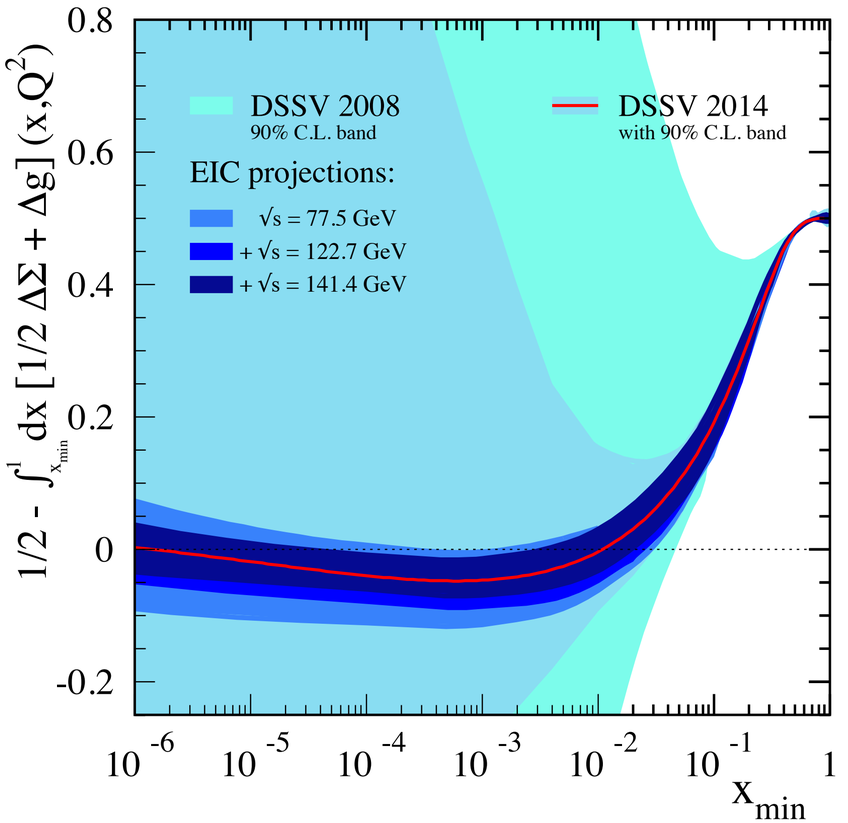

$$\Delta q(x) = \frac{1}{4\pi}\int dy^- e^{-ixp^+y^-}\langle P,S|\bar{\psi}(0,y^-,0_\perp)\gamma^+\gamma_5\psi(0)|P,S\rangle$$

$$\Delta\Sigma(Q^2) = \sum_q^{N_f}\int_0^1 dx\left(\Delta q(x,Q^2)+\Delta\bar{q}(x,Q^2)\right)$$

$$\Delta q(x) =$$

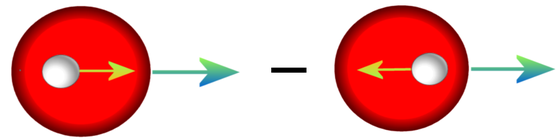

Parton distributions on the lattice

Lattice QCD: calculation of physical observables from the path integral in Euclidean space

Quasi-PDFs can be calculated on the lattice, large-momentum effective theory (LaMET)

$$\tilde{q}(x,\mu^2,P^z) = \int \frac{dz}{4\pi} e^{izk^z} \langle P|\bar{\psi}(z)\gamma^z \exp\Big(-ig\int_0^z dz' A^z(z')\Big)\psi(0)|P\rangle$$

J. Xi (2013)

and related to “physical” distributions

$$\tilde{q}(x,\mu^2,P^z) = \int_{-\infty}^{\infty} \frac{dy}{|y|} C(\frac{x}{y},\frac{\mu}{P_z}) q(y,\mu) + \mathcal{O}\Big(\frac{M_N^2}{P_z^2}, \frac{\Lambda_{QCD}^2}{(xP_z)^2}, \frac{\Lambda_{QCD}^2}{\big((1-x)P_z\big)^2}\Big)$$

better signal with $P_z \to \infty$ but large uncertainties

Xiong, Ji, Zhang, Zhao (2013)
Chen, Cohen, Ji, Lin, Zhang (2016)

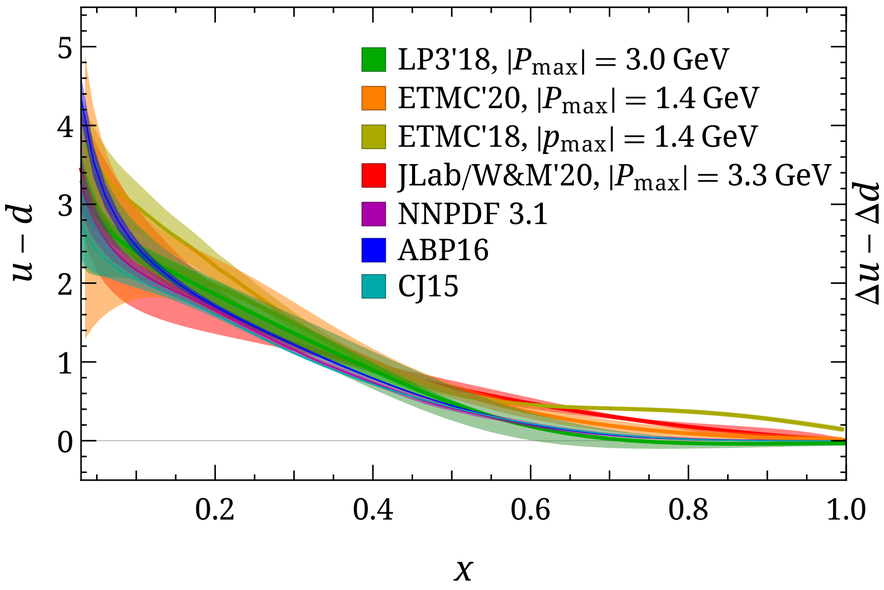

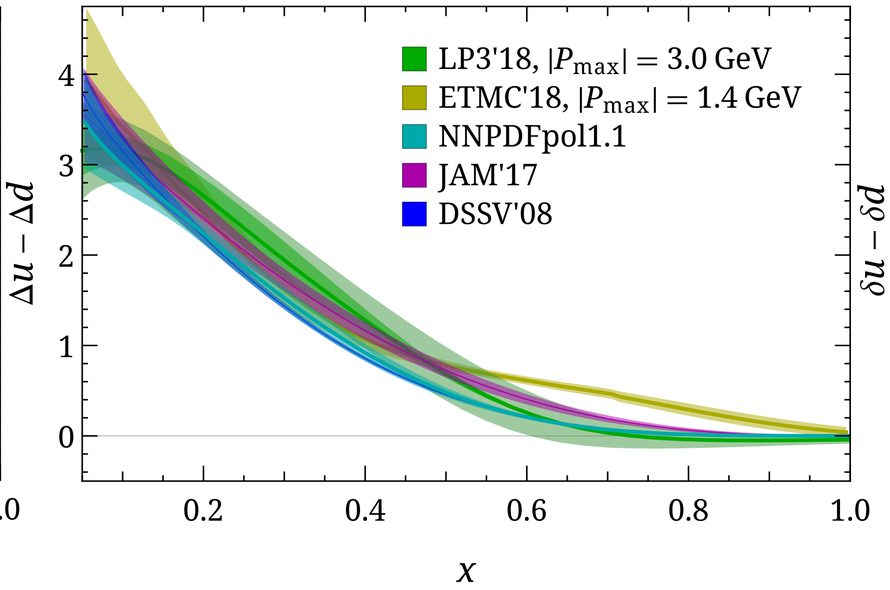

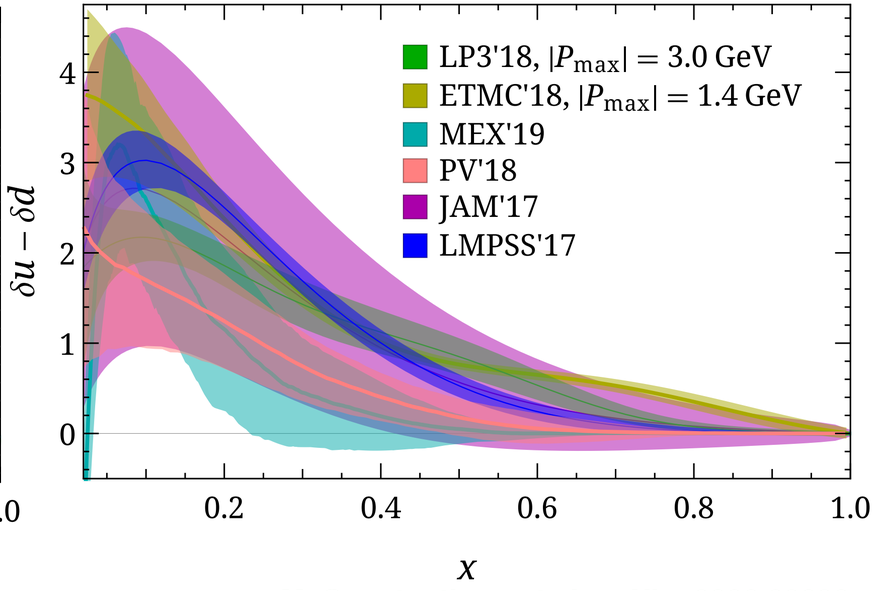

M. Constantinou et al., arXiv: 2006.08636

Parton distributions on the lattice: beyond PDFs

Quantities calculable on the lattice = Perturbative kernel ⊗ PDFs, TMDs, GPDs, etc.

Various methods and schemes: Quasi-PDFs (X. Ji, 2013), Pseudo-PDFs (A. Radyushkin, 2017), Compton amplitude method (A. Chambers et al., 2017), Lattice cross-section method (Y. Ma and J. Qiu, 2014), Hadronic tensor currents (K.-F. Liu, 2016), quasi-GPDs (Ji et al., 2015; Liu et al., 2019), pseudo-GPDs (Radyushkin, 2019), quasi-TMDs (Ebert et al., 2019) etc.

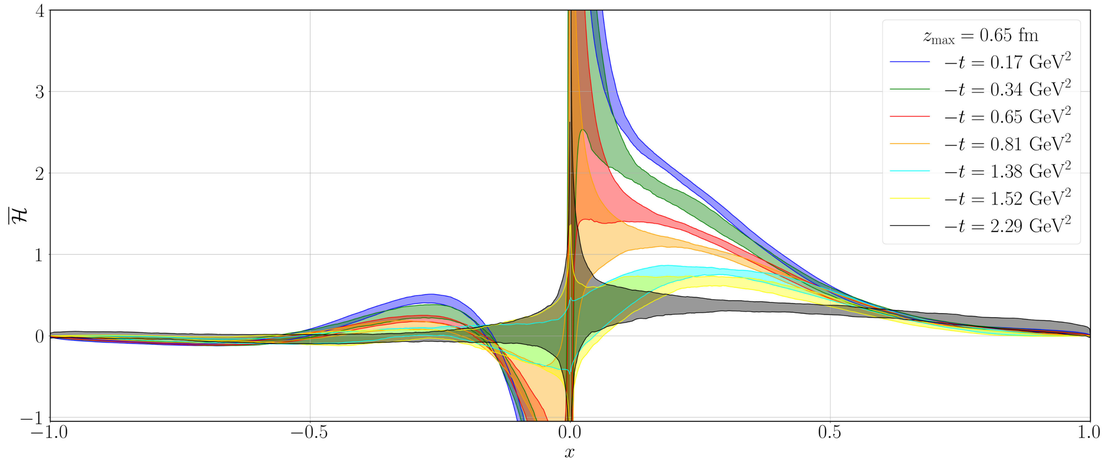

Bhattacharya et al., (2024)

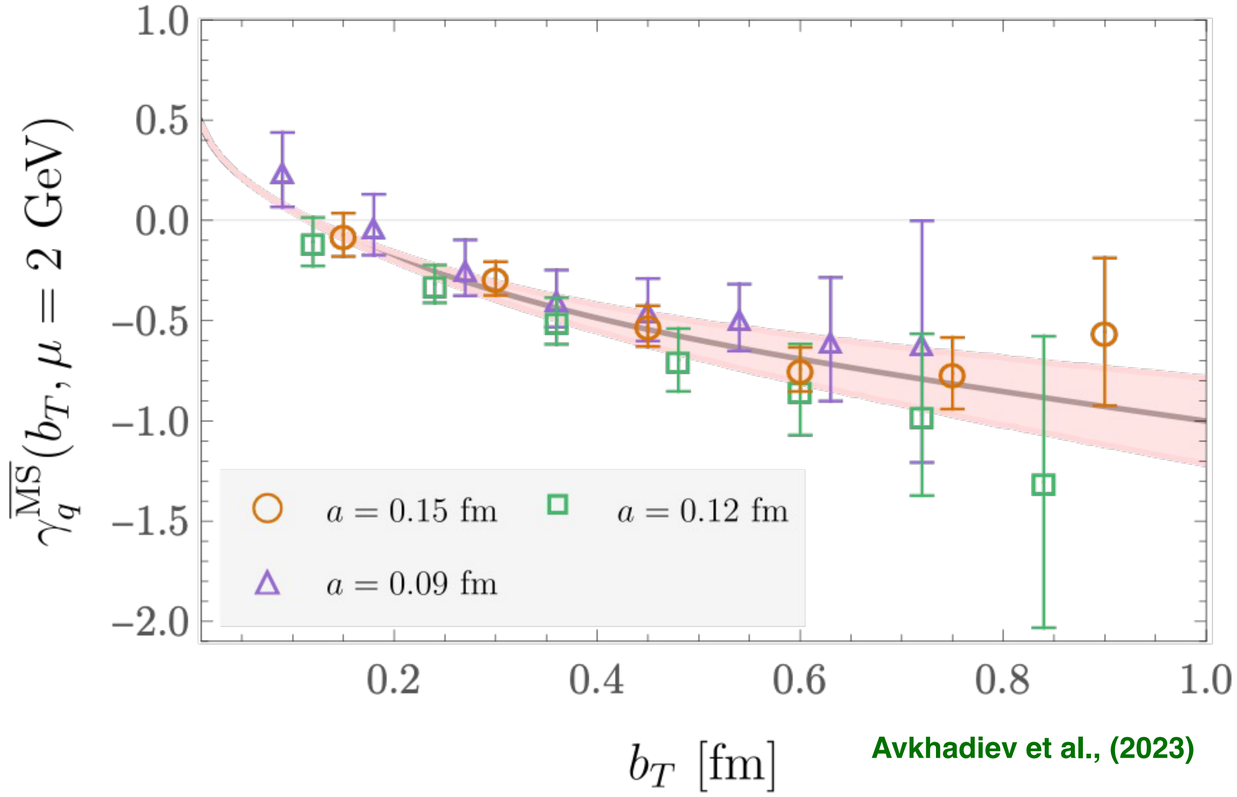

Avkhadiev et al., (2023)

Global analysis of PDFs with lattice data

C. Egerer et al., (2022)

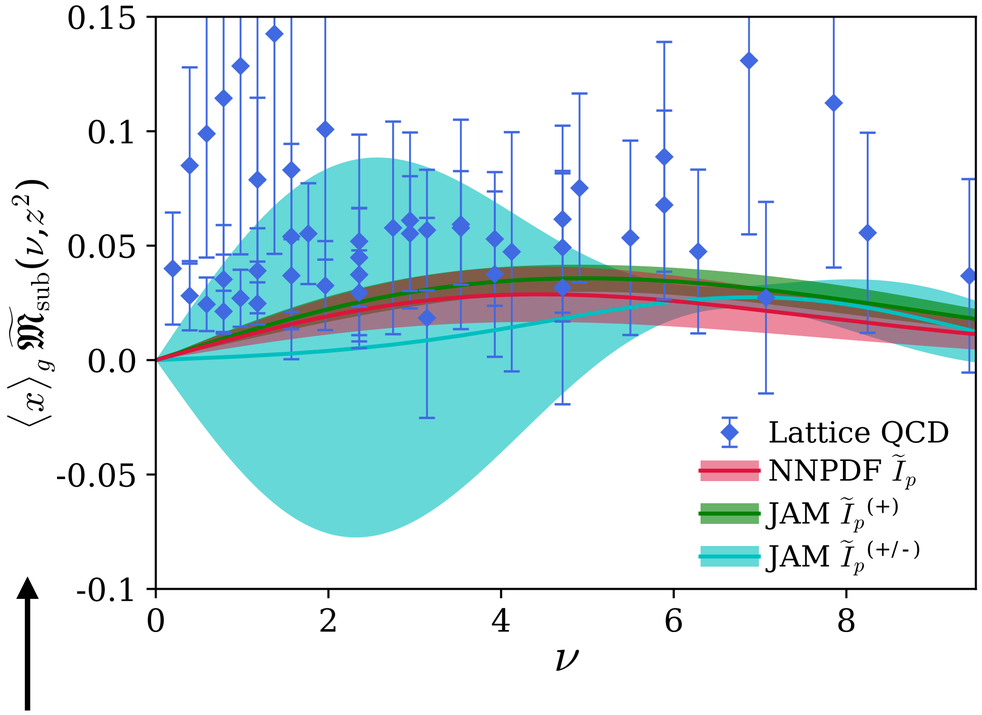

Lattice matrix element depending on the pseudo-distribution

$$\tilde{\mathcal{I}}_p(\nu) = \frac{i}{2}\int_{-1}^{1} dx e^{-ix\nu} x\Delta g(x)$$

Lattice results can be used to support phenomenology of experimental data at EIC

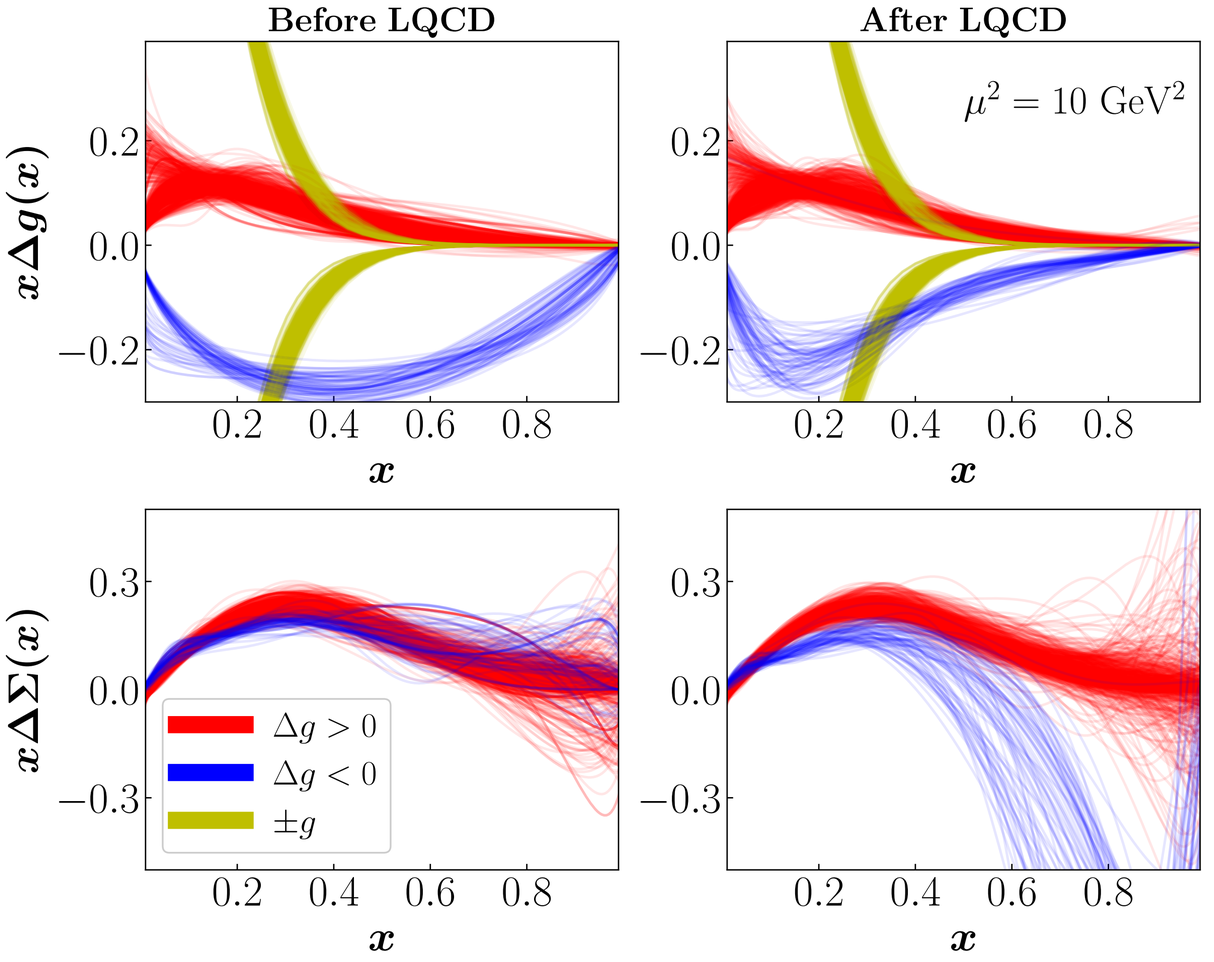

J. Karpie et al., (2023)

Transverse momentum dependent distributions (TMDPDFs)

The transverse momentum dependent (TMD) factorization scheme can be used for analysis of scattering with production of a final state with transverse momentum $P_\perp$ which is much smaller than a hard scale

$$P_\perp^2/Q^2 \ll 1 \Rightarrow b_\perp \lesssim \Lambda_{QCD}^{-1}$$

$$\frac{d\sigma^{\text{SIDIS}}}{dxdzdq_\perp dQ} \propto x\mathcal{H}^{\text{SIDIS}}(Q,\mu)\sum_a e_a^2 \int d^2k_\perp \int \frac{d^2P_\perp}{z^2} f_1^a(x,k_\perp^2;\mu,\zeta_A) D_1^{a\to h}(z,P_\perp^2;\mu,\zeta_B)$$

- The TMDPDFs depend on two factorization scales (μ and ζ) which define separation of the dynamic modes in the TMD factorization scheme → different types of emission

$$\frac{d}{d\ln\mu} f_i(x,b_\perp,\mu,\zeta) = \gamma_\mu^i(\mu,\zeta) f_i(x,b_\perp,\mu,\zeta)$$

$$\frac{d}{d\ln\zeta} f_i(x,b_\perp,\mu,\zeta) = \frac{1}{2}\gamma_\zeta^i(\mu,b_\perp) f_i(x,b_\perp,\mu,\zeta)$$

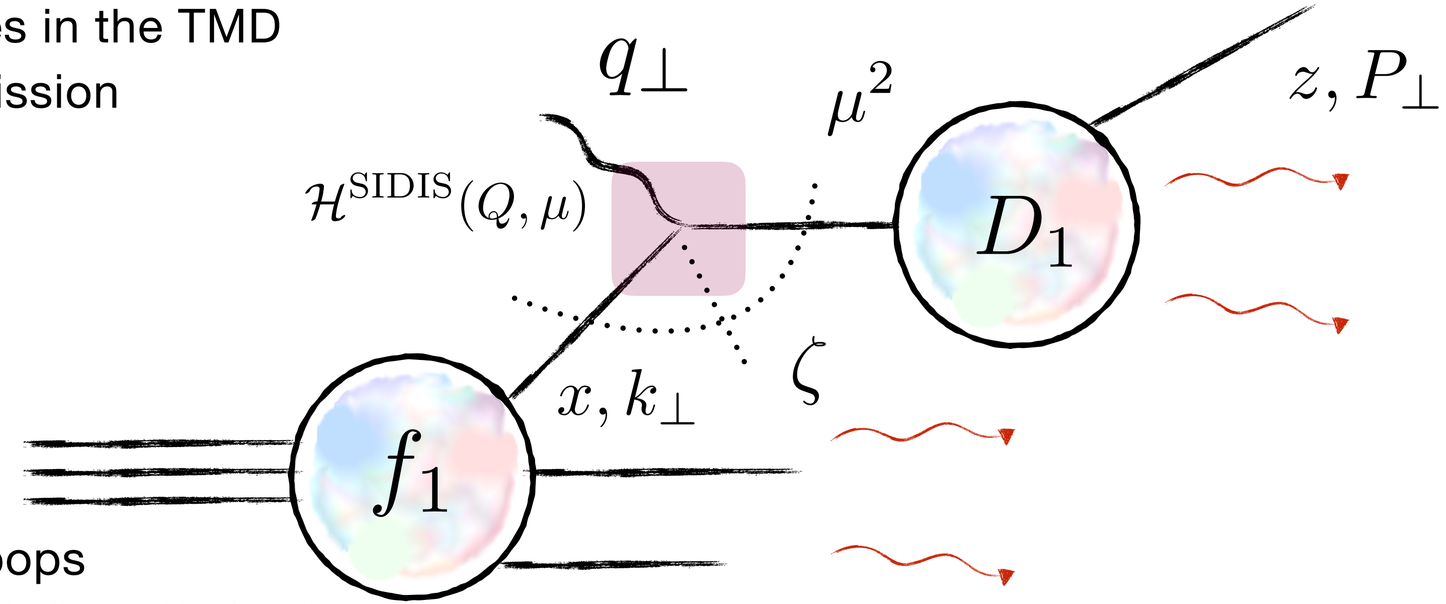

The anomalous dimensions are known up to 4 loops

Duhr, Mistlberger, Vita (2022)
Manteuffel, Panzer, Schabinger (2020)

TMD global analysis

	Framework	W+Y	HERMES	COMPASS	DY	Z boson	W boson	N of points
KN 2006 hep-ph/0506225	LO-NLL	W	✘	✘	✔	✔	✘	98
QZ 2001 hep-ph/0506225	NLO-NLL	W+Y	✘	✘	✔	✔	✘	28 (?)
RESBOS resbos@msu	NLO-NNLL	W+Y	✘	✘	✔	✔	✘	>100 (?)
Pavia 2013 arXiv:1309.3507	LO-PM	W	✔	✘	✘	✘	✘	1538
Torino 2014 arXiv:1312.6261	LO-PM	W	✔ (separately)	✔ (separately)	✘	✘	✘	576 (H) 6284 (C)
DEMS 2014 arXiv:1407.3311	NLO-NNLL	W	✘	✘	✔	✔	✘	223
EIKV 2014 arXiv:1401.5078	LO-NLL	W	1 (x,Q^2) bin	1 (x,Q^2) bin	✔	✔	✘	500 (?)
SIYY 2014 arXiv:1406.3073	NLO-NLL	W+Y	✘	✔	✔	✔	✘	200 (?)
Pavia 2017 arXiv:1703.10157	LO-NLL	W	✔	✔	✔	✔	✘	8059
SV 2017 arXiv:1706.01473	NNLO-NNLL	W	✘	✘	✔	✔	✘	309
BSV 2019 arXiv:1902.08474	NNLO-NNLL	W	✘	✘	✔	✔	✘	457
Pavia 2019 arXiv:1912.07550	NNLO-N3LL	W	✘	✘	✔	✔	✘	353
SV 2019 arXiv:1912.06532	NNLO-N3LL	W	✔	✔	✔	✔	✘	1039
MAP pion 2022 arXiv:2210.01733	NLO-N3LL	W	✘	✘	✔	✘	✘	138
MAP 2022 arXiv:2206.07598	NNLO-N3LL-	W	✔	✔	✔	✔	✘	2031
JAM 2023 arXiv: 2302.01192	NLO-NNLL	W	✘	✘	✔	✘	✘	608
ART 2023 arXiv:2305.07473	N3LO-N4LL	W	✘	✘	✔	✔	✔	627
Aslan at al 2024 arXiv:2401.14266	NLO-NLL	W	✘	✘	✔	✘	✘	130
MAP 2025 arXiv:2502.04166	NNLO-N3LL	W	✘	✘	✔	✔	✘	482

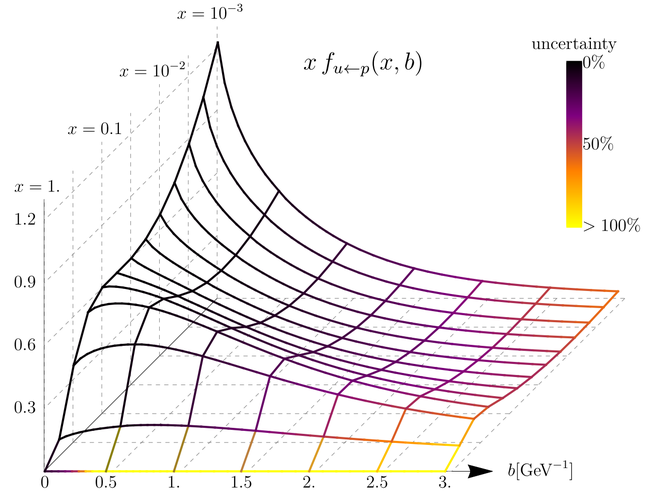

Moos, Scimemi, Vladimirov, Zurita (2023)

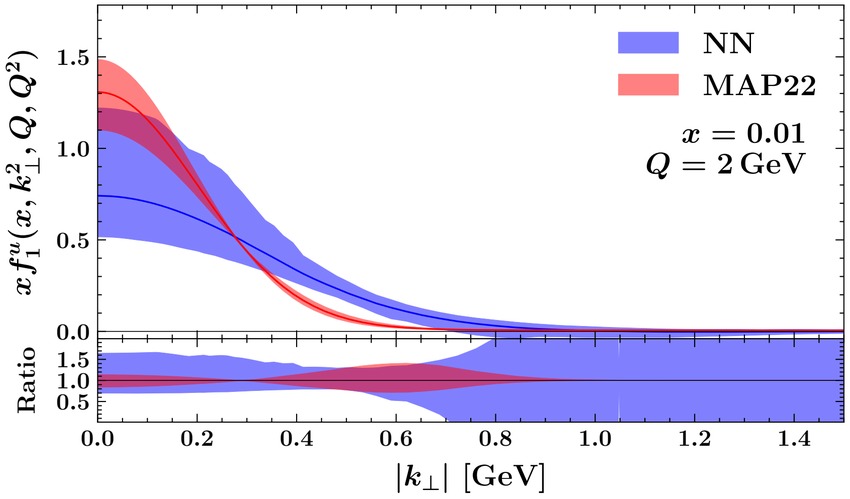

Bacchetta, Bertone, Bissolotti, Cerutti, Radici, Rodini, Rossi (2025)

Global analysis is important for testing universality of distributions

Significant progress in the TMD phenomenology, that will flourish in the EIC era

Power corrections to the TMD factorization

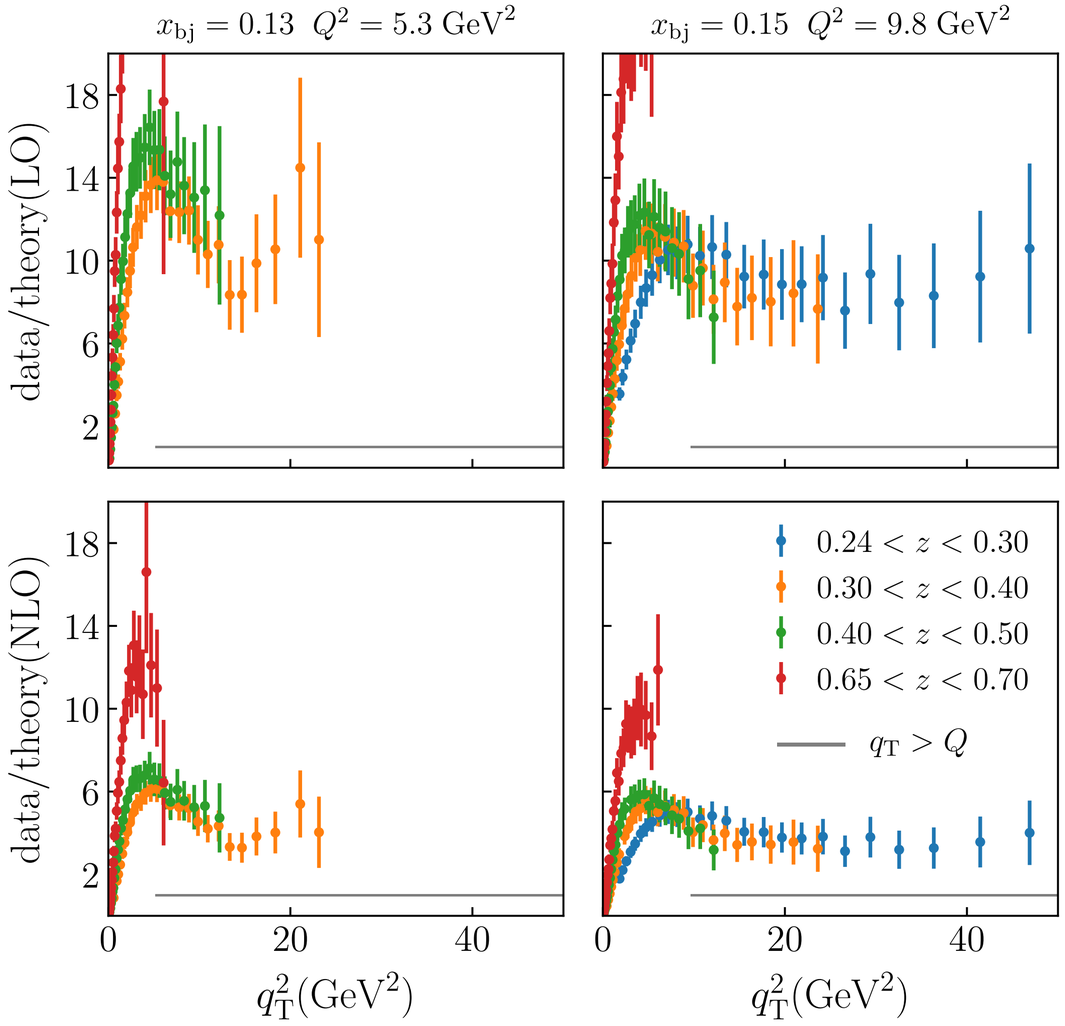

Gonzalez-Hernandez, Rogers, Sato, Wang (2018)

TMD formalism doesn't work in the region of large $q_\perp$ or small $b_\perp$

The TMD factorization approach is valid in the region of small $q_\perp$ or large $b_\perp$

To minimize power corrections to the TMD factorization formula the data cuts $q_\perp/Q < 0.25$ are implemented

To cover large $q_\perp$ data we need to include power corrections in the analysis (Balitsky, Tarasov, 2017; Liu, Qiu, 2020; Vladimirov, 2023)

leading order TMD factorization

power corrections

$$W(\alpha_z,\beta_z,q_\perp) \simeq -\frac{e^2}{8s_W^2c_W^2N_c}\int d^2k_\perp \frac{1}{k_\perp^2(q-k)_\perp^2}\left[1-2\frac{(k,q-k)_\perp}{Q^2}\right]$$
$$\times\left[\left\{(1+a_u^2)[f_u(\alpha_z)\bar{f}_u(\beta_z)+\bar{f}_u(\alpha_z)f_u(\beta_z)]\right\}+\left\{u\leftrightarrow c\right\}+\left\{u\leftrightarrow d\right\}+\left\{u\leftrightarrow s\right\}\right]$$

Balitsky, Tarasov (2018)

Power corrections for Z-boson production

Collinear matching

- $f_i(x, b_\perp, \mu, \zeta)$ term is intrinsically non-perturbative and extraction of its perturbative component (dependence on the factorization scales μ and ζ) is complicated. Function of four variables!
- The TMDPDFs has been directly calculated only in the region of small $b_\perp$
- The conventional approach is to consider a TMDPDF in a small $b_\perp \ll \Lambda_{QCD}^{-1}$ approximation and expand it in terms of the collinear PDFs - collinear matching: see e.g. Scimemi, Tarasov and Vladimirov (2019)

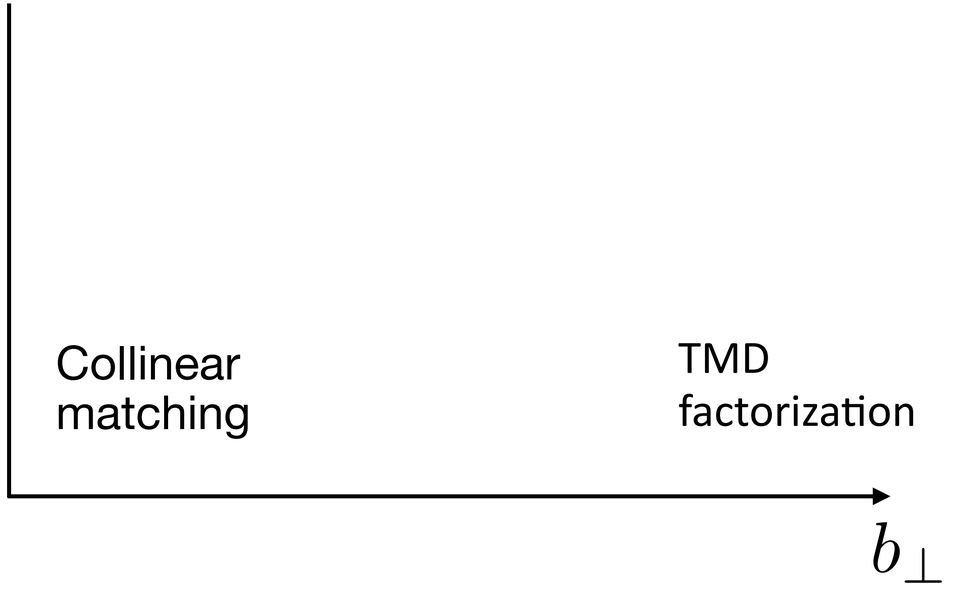

$$f_i(x, b_\perp, \mu, \zeta) = C_1 \otimes f_1(x, \mu) + b_\perp^2 C_2 \otimes f_2(x, \mu) + \dots$$

Matching coefficients (perturbative), contains logs of IR origin

Collinear PDFs of rising twist

- However, the region of applicability of the TMD factorization corresponds to large $b_\perp \lesssim \Lambda_{QCD}^{-1}$. The TMDPDFs genuinely contain contribution of all collinear twists!

Problem: Only first few terms of the collinear matching are known. To obtain the correct structure of the TMDPDFs, which describes all collinear twist content of the distributions, one would need to resum all terms of the collinear expansion, which at the moment is not feasible!

TMD in the Collins-Soper-Sterman (CSS) framework

- In practice a phenomenological solution is used: higher twist terms are dropped

$$f_i(x, b_\perp, \mu, \zeta) = C_1 \otimes f_1(x, \mu) + \cancel{b_\perp^2 C_2 \otimes f_2(x, \mu) + \dots}$$

- In this approximation only leading twist-content of the TMD distribution is taken into account with the double logarithmic CSS evolution and IR logarithms of the DGLAP type (leading twist large-x evolution)

$$f(x_B, b_\perp, \mu, \zeta) = f_1(x_B, 0_\perp, \mu) - \frac{\alpha_s N_c}{\pi} L_b^\mu \int_0^1 \frac{dz}{z} P_{gg}(z) f(\frac{x_B}{z}, 0_\perp, \mu)$$

$$+ \frac{\alpha_s N_c}{2\pi} \Big(-\frac{1}{2}(L_b^\mu)^2 + L_b^\mu \ln \frac{\mu^2}{\zeta^2} - \frac{\pi^2}{12} \Big) f(x_B, 0_\perp, \mu) + \dots$$

DGLAP

CSS evolution

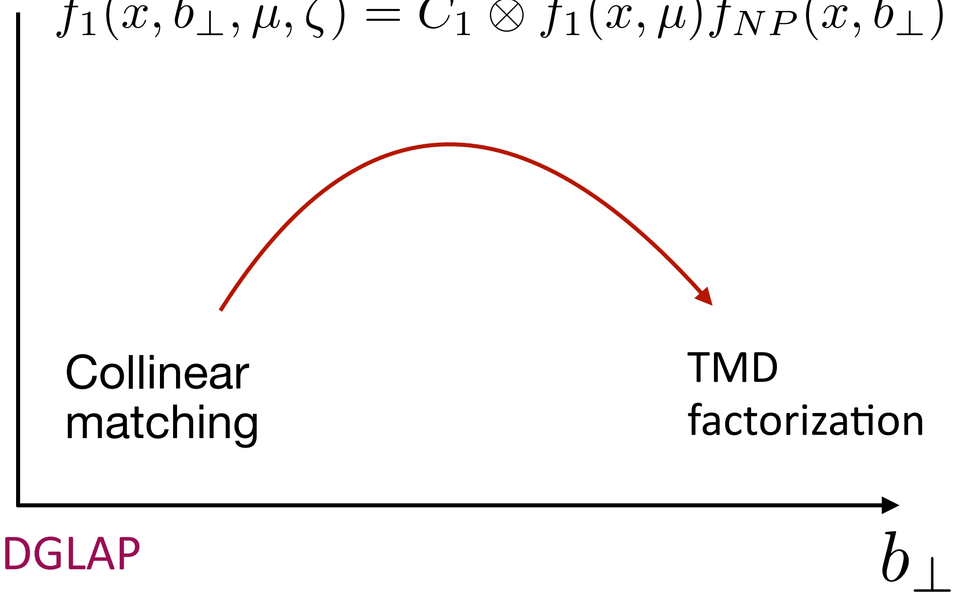

In particular, no signs of the small-x physics (all-twist resummation)

- A phenomenological ansatz f_{NP} is introduced to extrapolate the result from $b_\perp \ll \Lambda_{QCD}^{-1}$ into the physical region $b_\perp \lesssim \Lambda_{QCD}^{-1}$

The procedure doesn't allow us to reveal all collinear twist content of the TMDPDFs which is important in the region of applicability of the TMD factorization

Collinear vs. TMD factorization

The collinear matching "model" for unpolarized TMDPDF used in the phenomenology:

TMD distribution for the small $q_\perp$ region

$$\hat{f}_1^a(x, b_\perp^2; \mu_f, \zeta_f)$$
$$= [C \otimes f_1](x, b_*; \mu_{b_*}, \mu_{b_*}^2) \exp\left\{ \int_{\mu_{b_*}}^{\mu_f} \frac{d\mu}{\mu} \gamma(\mu, \zeta_f) \right\} \left(\frac{\zeta_f}{\mu_{b_*}^2} \right)^{K(b_*, \mu_{b_*})/2} f_{1\mathrm{NP}}(x, b_\perp^2; \zeta_f, Q_0)$$

Collinear matching constructed in the region of large $q_\perp$

CSS evolution

Phenomenological function encompassing all-collinear twist content of the distribution

TMD factorization ≠ collinear factorization

The discrepancies between collinear and TMD factorizations manifest themself in the phenomenology:

$$\frac{d\sigma_\omega^{\mathrm{SIDIS}}}{dx\, dz\, d|\boldsymbol{q}_T|\, dQ} = \omega(x, z, Q) \frac{d\sigma^{\mathrm{SIDIS}}}{dx\, dz\, d|\boldsymbol{q}_T|\, dQ}$$

At NLL, $\omega(x, z, Q) = 1$. Beyond NLL, the prefactor becomes larger than one and guarantees that the integral of the TMD part of the cross section reproduces most of the collinear cross section, as suggested by the data.

Bacchetta, Bertone, Bissolotti, Bozzi, Cerutti, Piacenza, Radici, Signori (2022)

Can we better address the all-collinear twist content of the TMDPDFs?

TMDPDFs in the region of small $q_\perp$

- The TMDPDFs can be calculated directly in the region of applicability of the TMD factorization: region of small $q_\perp$ or large $b_\perp \lesssim \Lambda_{QCD}^{-1}$
- The structure of TMDPDFs in this region is rich and goes beyond the leading-twist collinear contribution

$$f(x_B, b_\perp, \mu^2_{\rm UV}, \zeta) = f(x_B, b_\perp, \mu^2_{\rm IR}, \rho) - \frac{\alpha_s N_c}{\pi} L_b^{\mu_{\rm IR}} \int_0^1 \frac{dz}{z} \mathcal{P}_{gg}(z) f(\frac{x_B}{z}, b_\perp, \mu^2_{\rm IR}, \rho)$$

DGLAP IR logs

$$+ \frac{\alpha_s N_c}{2\pi} \Big(-\frac{1}{2} (L_b^{\mu_{\rm UV}})^2 + L_b^{\mu_{\rm UV}} \ln \frac{\mu^2_{\rm UV}}{\zeta^2} - \frac{\pi^2}{12} \Big) f(x_B, b_\perp, \mu^2_{\rm IR}, \rho)$$

CSS evolution

$$- \frac{\alpha_s N_c}{2\pi} \int \text{đ}^2 p_\perp e^{ip_\perp b_\perp} \Big(\frac{1}{2} \ln^2 \frac{\mu^2_{\rm IR}}{p_\perp^2} + \ln \frac{\mu^2_{\rm IR}}{p_\perp^2} \ln \frac{\rho}{\zeta} - \frac{\pi^2}{12} \Big) f(x_B, p_\perp, \mu^2_{\rm IR}, \rho)$$

BFKL-like IR logs

$$+ \frac{\alpha_s N_c}{2\pi} \int d^2 z_\perp \int \text{đ}^2 p_\perp e^{ip_\perp (b-z)_\perp} \Big(\frac{\beta_0}{2N_c} \ln \frac{\mu^2_{\rm UV}}{p_\perp^2} + \frac{67}{18} - \frac{5N_f}{9N_c} \Big) f(x_B, z_\perp, \mu^2_{\rm IR}, \rho) + \dots$$

Mukherjee, Skokov, Tarasov, Tiwari (2024)

- The unpolarized gluon TMDPDF contains BFKL-like IR logarithms even in the region of large-x that reflect the all-collinear twist content of the TMDPDFs in the region of validity of the TMD factorization → observe these effects in TMD phenomenology, natural connection with small-x physics, e.g. initial conditions for the small-x evolution

Understanding the glue that binds us all

- What are the emergent properties of dense systems of gluons?

We aim to find the signatures of the gluon saturation at EIC in the region of small-x or eA scattering where the typical scale - the saturation scale - is enhanced as $Q_s^2 \propto A^{1/3}$

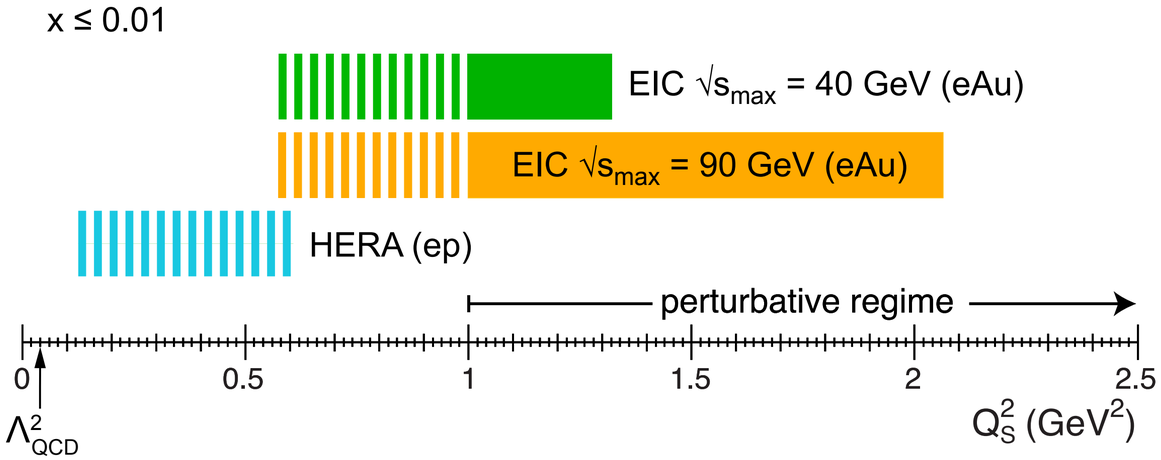

The emission is characterized by a strong ordering of the longitudinal momentum fraction

$$q^+ \ll k^+ \qquad q_\perp \sim k_\perp$$

→ large rapidity logarithms

$$\int^{1/x} \frac{dk^-}{k^-} \sim \ln 1/x$$

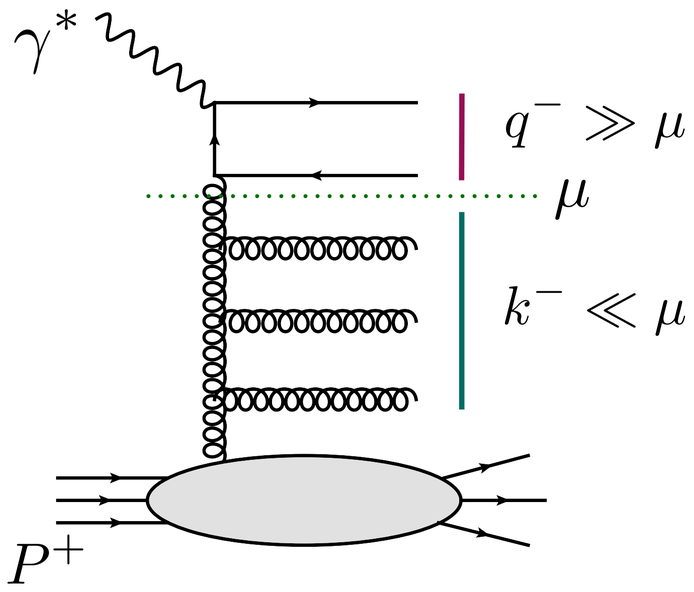

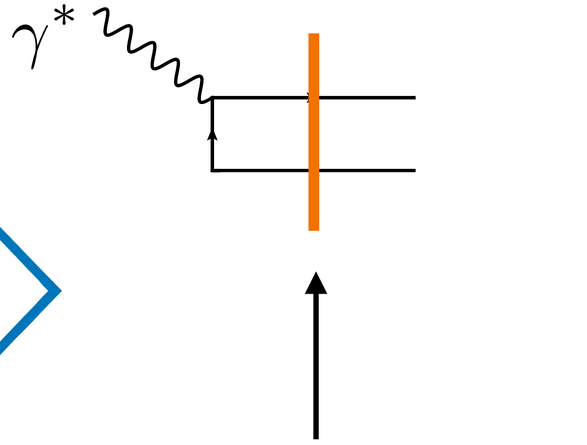

The target shrinks into the shock-wave background

Small-x physics at EIC: calculation of NLO corrections

Currently the research is focused on calculation of two types of “corrections” to the LO shock-wave picture. The first type is the NLO corrections

$$d\sigma = \mathrm{LO} + \mathrm{NLO}$$

α_s corrections

Precision small-x physics at EIC

Balitsky, Chirilli, 2008; Caron-Huot, Herranen, 2016; Chirilli, Xiao, Yuan, 2012; Boussarie, Grabovsky, Ivanov, Szymanowski, Wallon 2016; Iancu, Mulian 2021

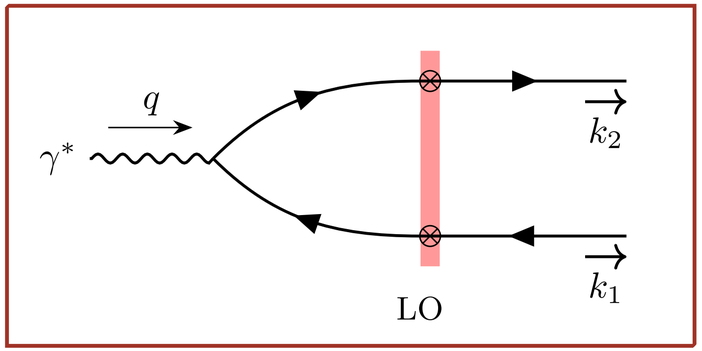

leading order (LO) contribution to the dijet production

Still some open questions: different schemes of resummation of DGLAP and Sudakov logs

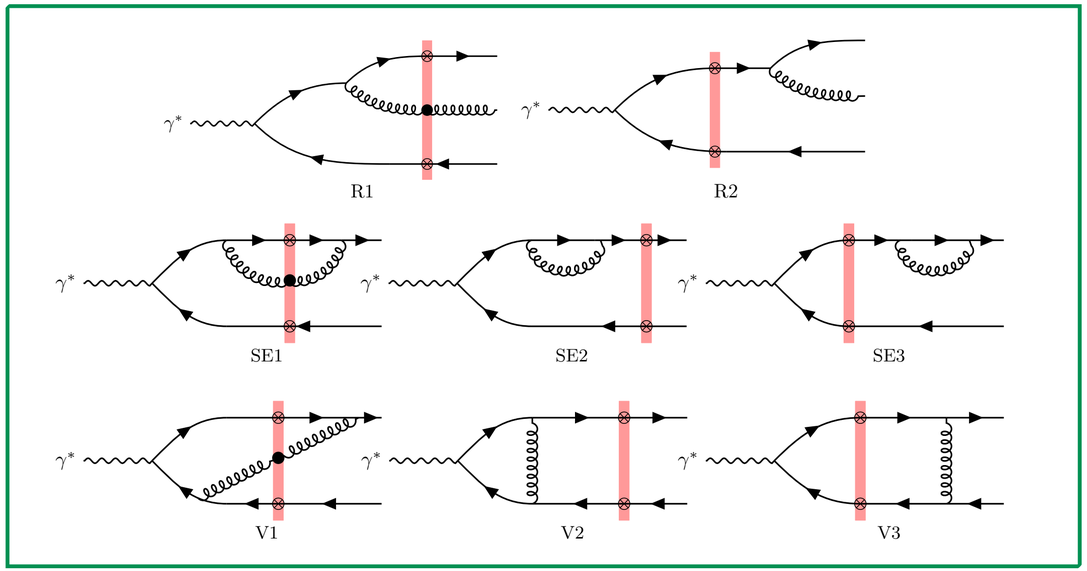

NLO corrections in the shock-wave picture of scattering

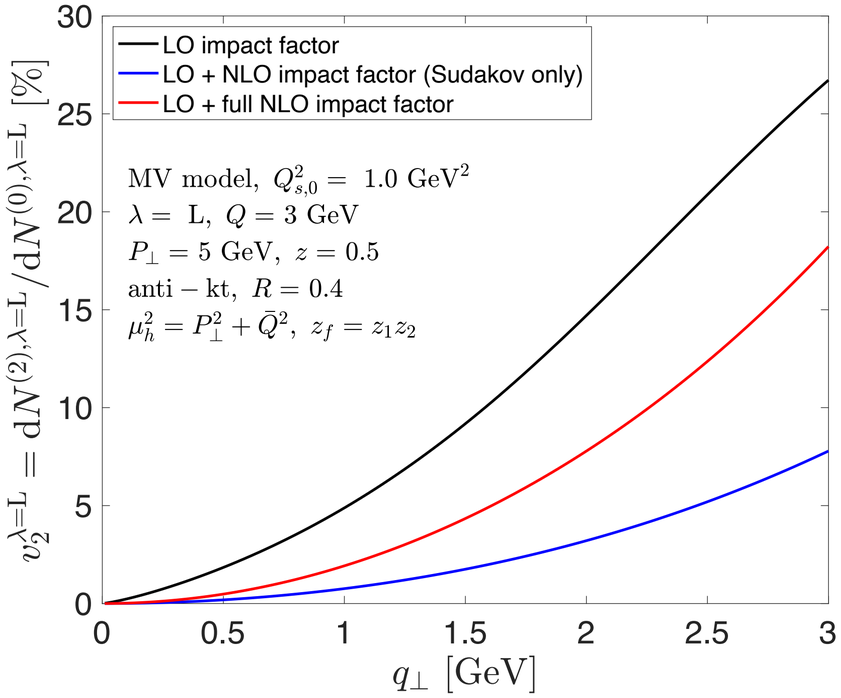

Caucal, Salazar, Schenke, Stebel, Venugopalan (2023)

Small-x physics at EIC: calculation of sub-ekonal corrections

The second type of correction - the sub-eikonal corrections - describe the corrections to the shock-wave picture of scattering

In the leading order (LO) shock-wave picture of scattering the interaction between factorized modes is instantaneous

$$d\sigma = \mathrm{LO} + \mathrm{NLO} + \mathrm{SubEik}$$

α_s corrections $1/s$ corrections

Altinoluk, Armesto, Beuf, Martínez, Salgado, 2014; Balitsky, Tarasov, 2015; Chirilli, 2019; Jalilian-Marian, 2019; Altinoluk and Beuf, 2022

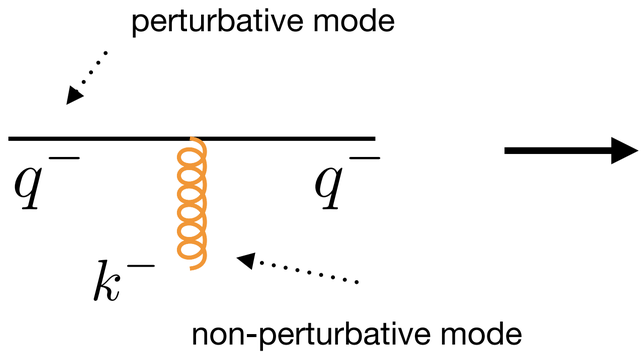

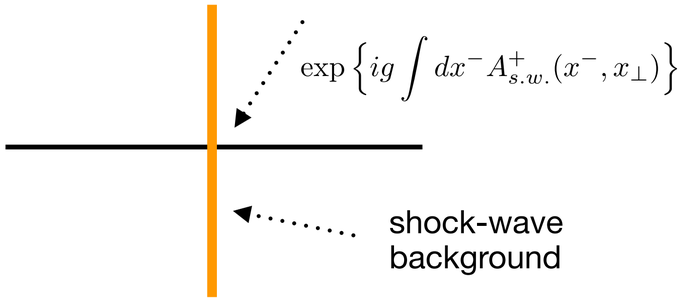

sub-eikonal corrections: internal structure of the shock-wave!

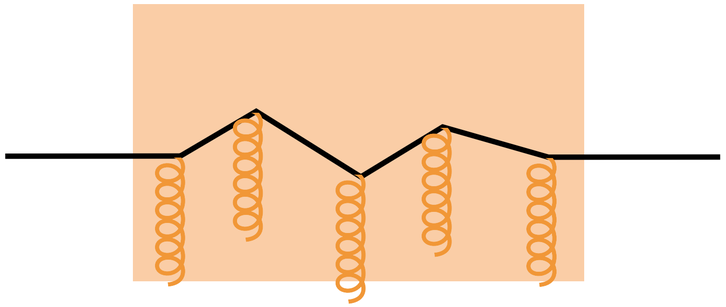

- How does the shock-wave decay? ⇒ large-x effects

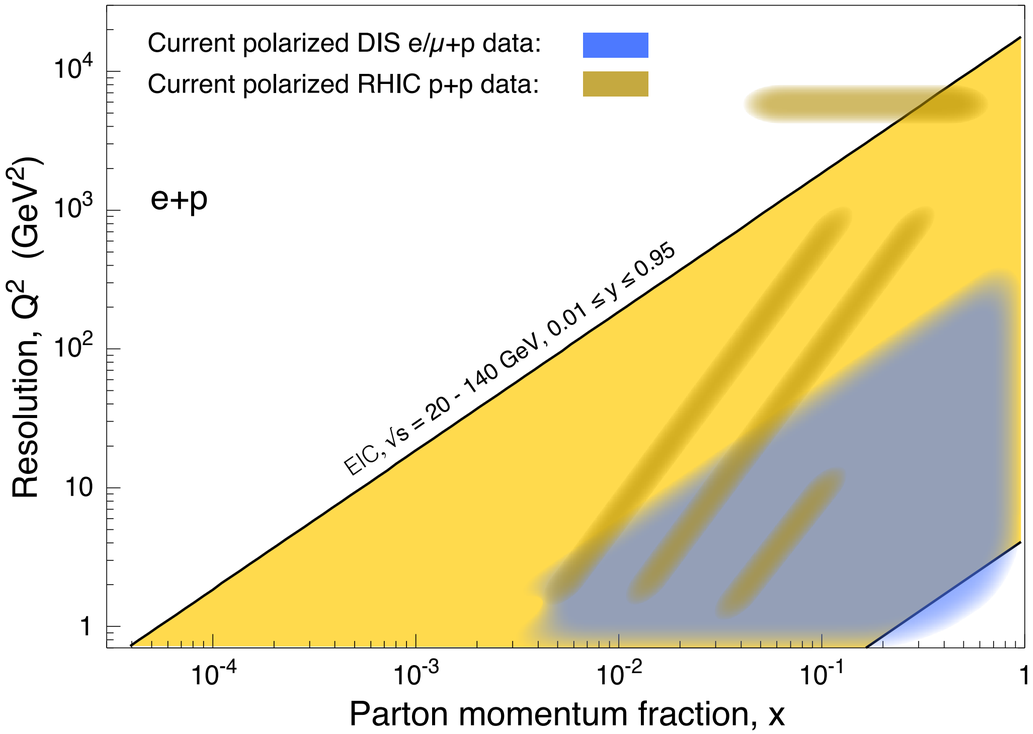

- Sub-eikonal effects dominate the region of moderate x (decay of the shock-wave)
- Sub-eikonal corrections are crucial for the search of saturation at EIC

The scattering at the sub-eikonal order

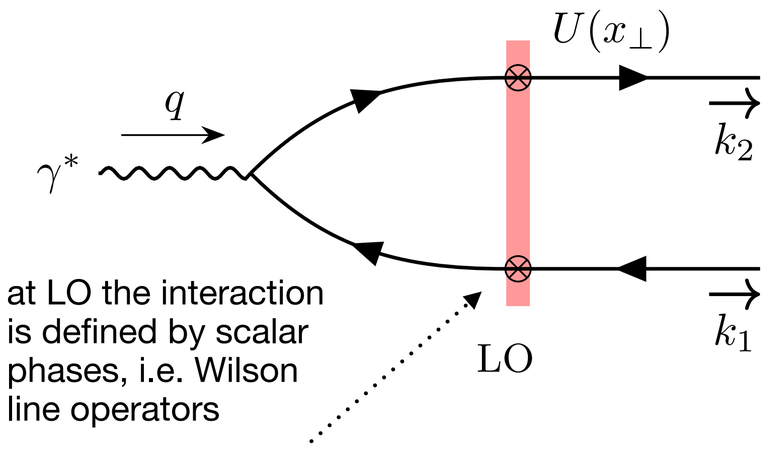

at LO the interaction is defined by scalar phases, i.e. Wilson line operators

$$U(y_\perp) \equiv \exp\left\{ig \int_{-\infty}^{\infty} dz^- A^+_{s.w.}(z^-, y_\perp)\right\}$$

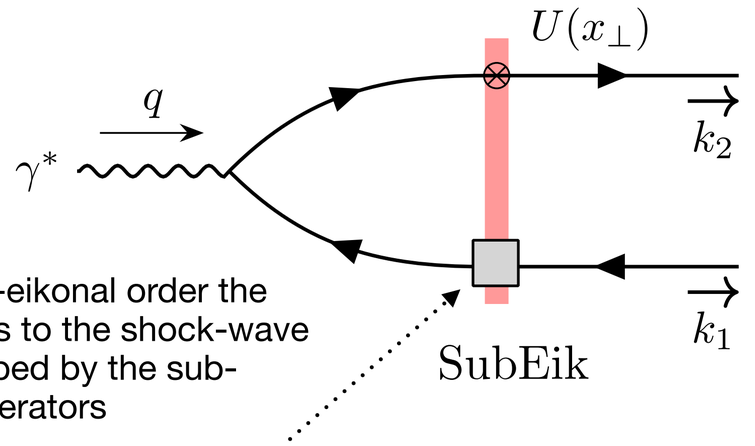

at the sub-eikonal order the corrections to the shock-wave are described by the sub-eikonal operators

$$U^{\text{sub-eik.}}(y_\perp) = ig \int_{-\infty}^{\infty} dz^- U_{[\infty,z^-]}(y_\perp) F_{12}(z^-, y_\perp) U_{[z^-,-\infty]}(y_\perp)$$

- The *scalar* phase at LO cannot describe spin effects ⇒ spin effects at small-x appear at sub-eikonal order
- Evolution properties of sub-eikonal operators are known ⇒ can construct predictions for observables

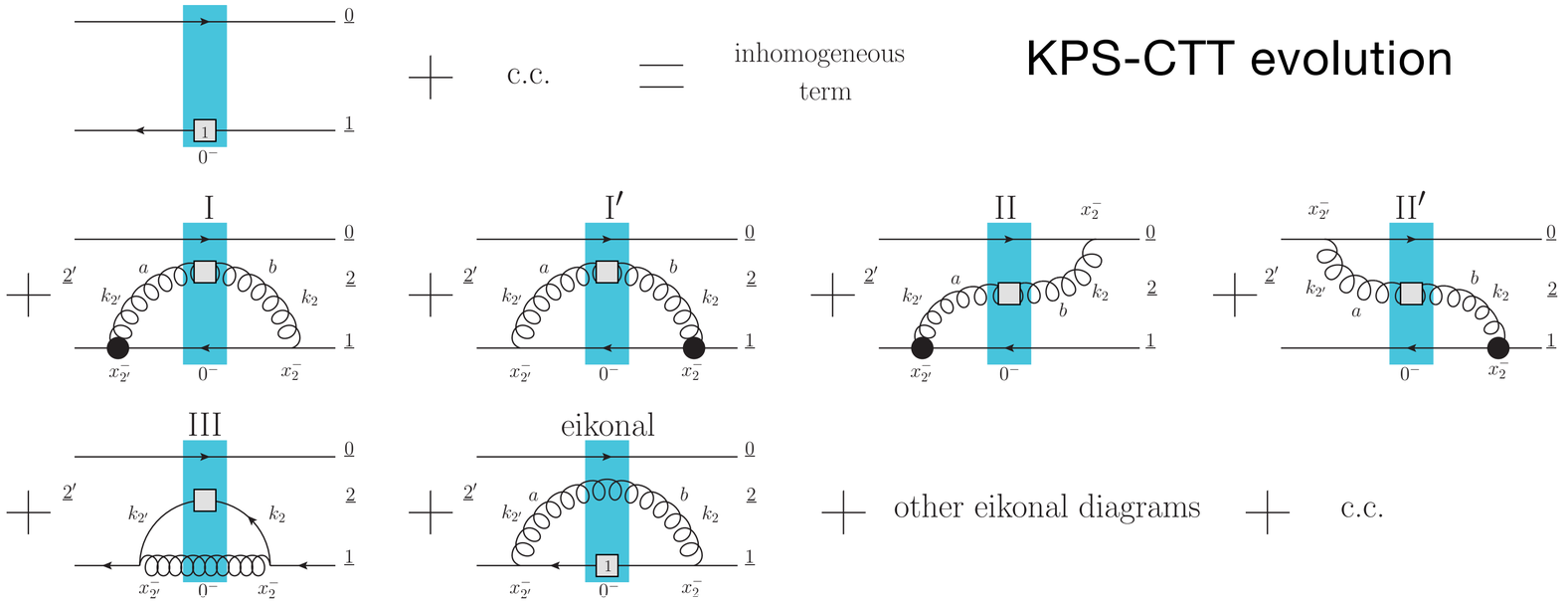

KPS-CTT evolution

Kovchegov, Pitonyak, Sievert, 2016; Cougoulic, Kovchegov, Tarasov, Tawabutr, 2022; Borden, Kovchegov, Li, 2023

How does the spin of the nucleon arise?

$$\frac{1}{2} = \frac{1}{2}\Delta\Sigma + \Delta G + L_q + L_g$$

huge uncertainty from the small-x region

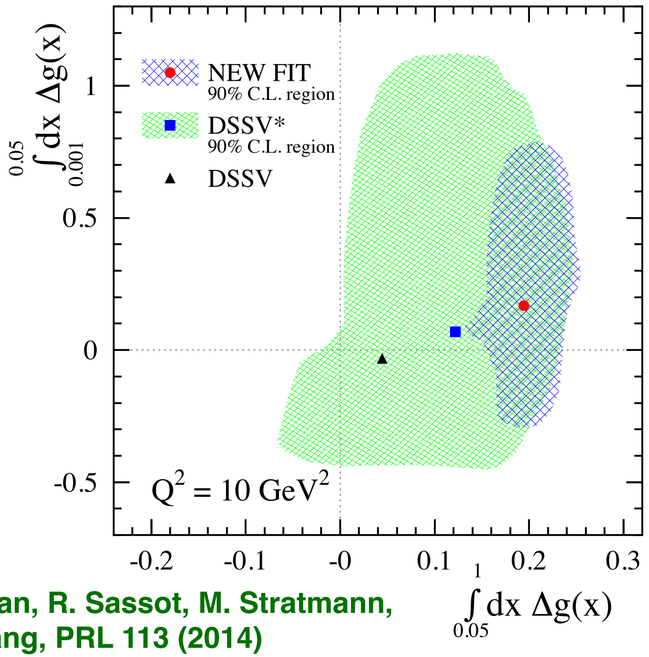

D. De Florian, R. Sassot, M. Stratmann, W. Vogelsang, PRL 113 (2014)

- In the small x region that cannot be probed experimentally, DGLAP-based predictions acquire a broad uncertainty band
- The benefit of small-x evolution is that it makes a genuine prediction for PDFs at small x given some initial conditions at a higher values of x

Initial condition at x_0

Small-x helicity evolution

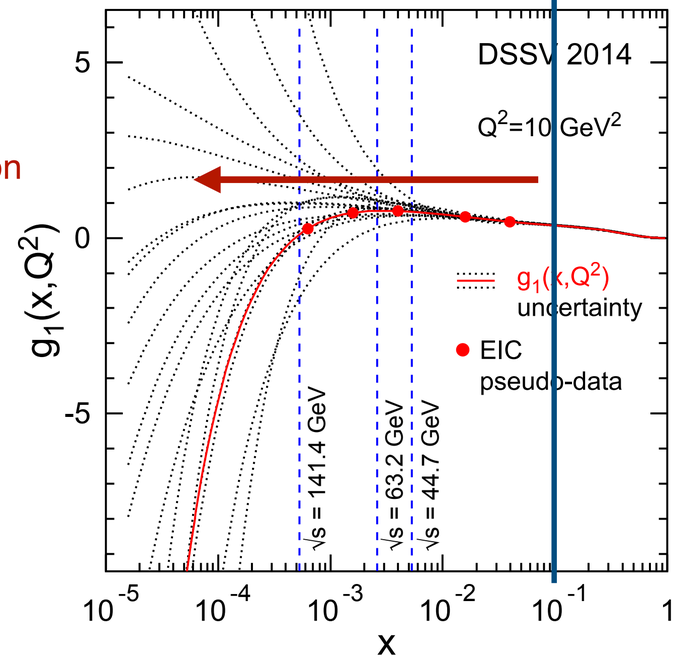

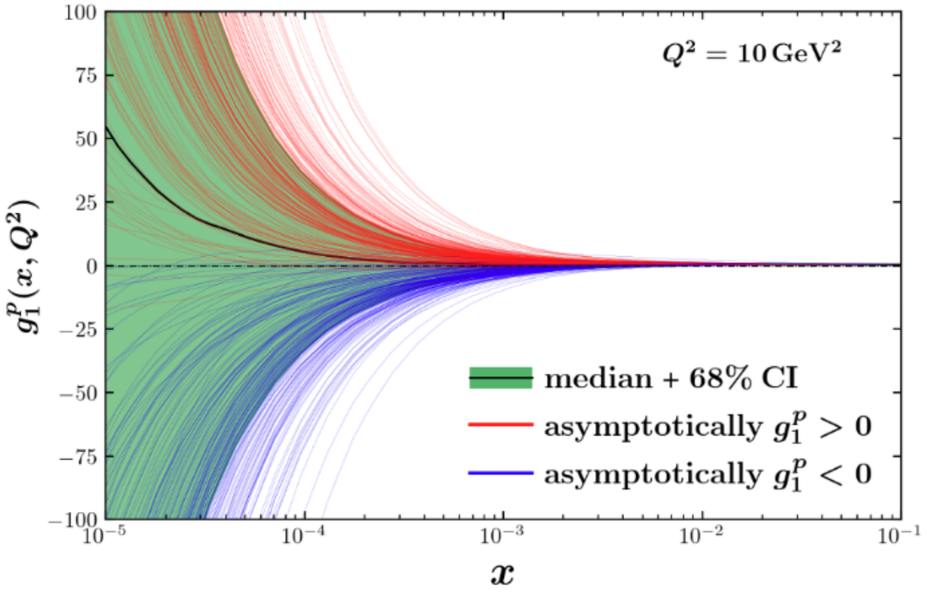

Baldonado et al., in preparation

All curves are defined by the same intercept

$$g_1(x,Q^2) \sim \left(\frac{1}{x}\right)^{\alpha_h}$$

The uncertainties are driven by the initial conditions ⇒ TMD physics can provide appropriate initial condition at large-x for the small-x evolution

Generalized parton distributions (GPDs)

GPDs can be extracted from the exclusive reactions, e.g. DVCS, DVMP

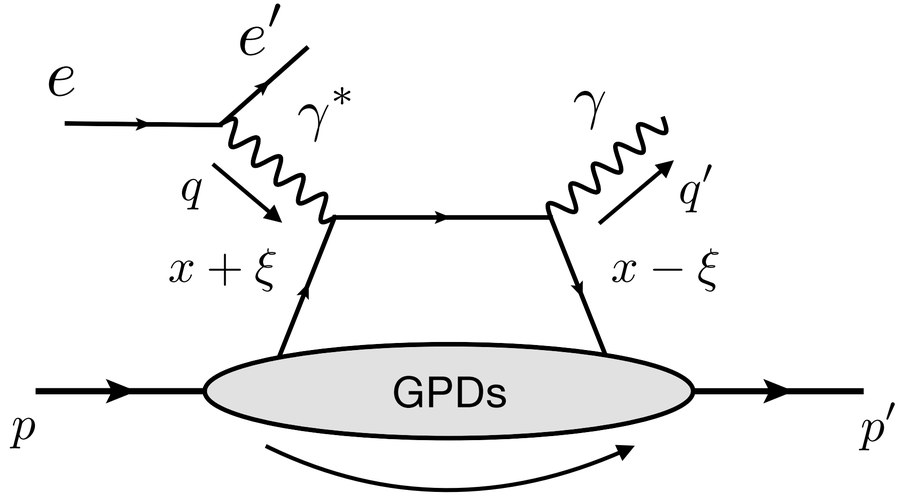

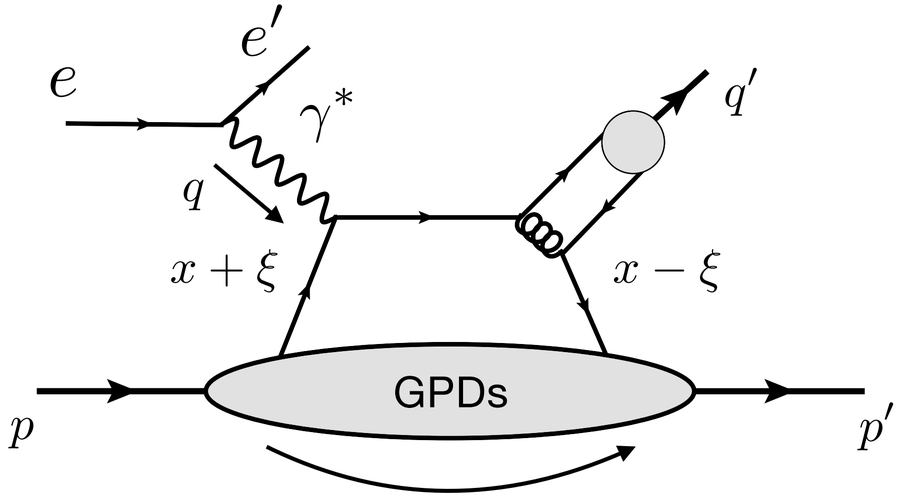

$$P = \frac{1}{2}(p+p') \qquad t = \Delta^2 \qquad p' - p = \Delta$$

$$t = \Delta^2$$

Aschenauer et al., 2025

Off-forward generalization of PDFs: Ji, 1997

$$P^+ \int \frac{dy^-}{2\pi} e^{ixP^+y^-} \langle p', s'|\bar{\psi}(0)\gamma^\mu \psi(y^-)|p,s\rangle$$

$$= H_q(x,\xi,t)\bar{u}(p',s')\gamma^\mu u(p,s) + E_q(x,\xi,t)\bar{u}(p',s')\frac{i\sigma^{\mu\nu}\Delta_\nu}{2M}u(p,s)$$

The Fourier transform with $\Delta_\perp$ yields distribution of partons in impact parameter space $b_\perp$, impact parameter distribution (IPD) Burkardt, 2000

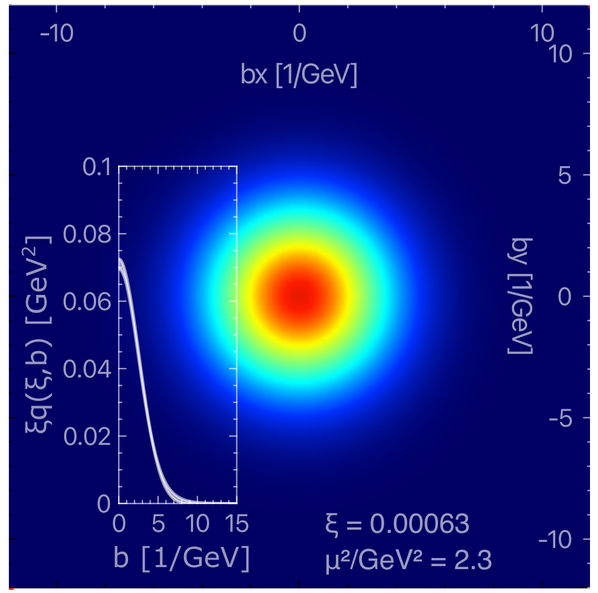

Extraction of GPDs

- Experimentally, GPDs are not well constraint. Can be extracted from Compton form factors (CFFs), but the extraction is not direct, hard to extract x-dependence:

$$\mathcal{F}(\xi,t) = \sum_q e_q^2 \int_{-1}^{1} dx \left(\frac{1}{\xi - x - i\epsilon} - \frac{1}{\xi + x - i\epsilon} \right) F^q(x,\xi,t)$$

$\mathcal{H}, \mathcal{E}$ CFF — H^q, E^q GPD

- The extraction can be simplified with some assumptions, e.g. dominance of the imaginary part of CFFs, constant skewness ξ, but the general analysis is complicated (satisfy polynomiality, positivity, evolution etc.)

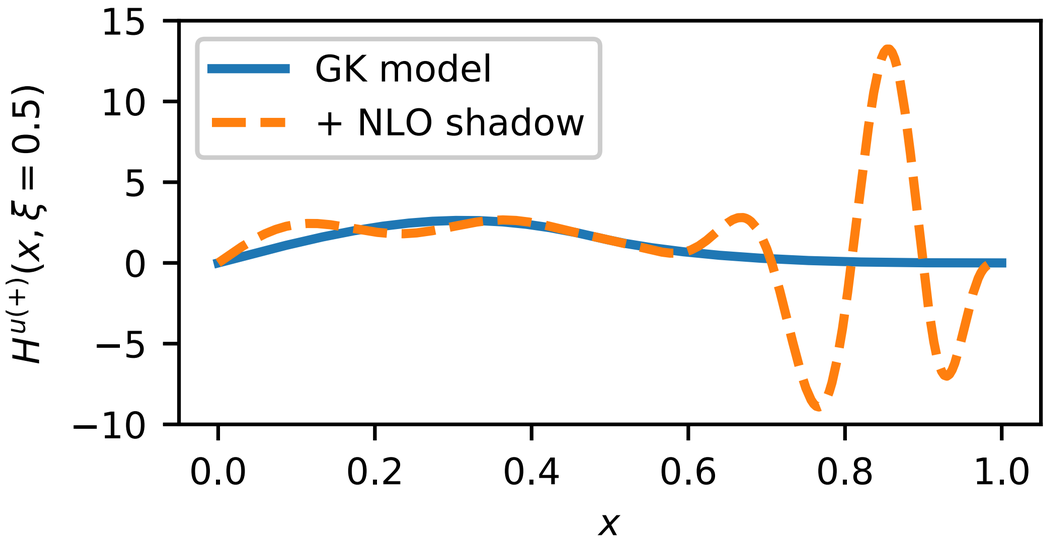

Bertone et al., 2021

- New physical processes for extracting GPDs: single diffractive hard exclusive processes (SDHEPs)

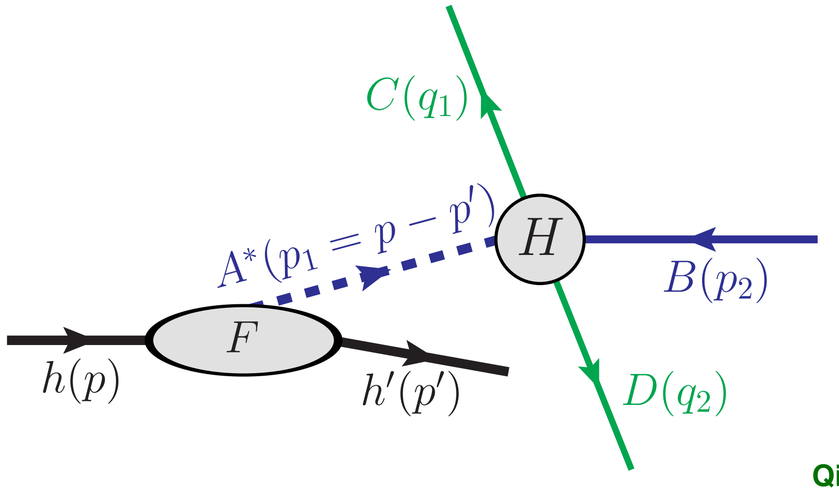

Qiu, Yu, 2023

The role of anomaly in GPDs and DIS structure functions

There are fundamental symmetries in QCD: the anomaly arises from the non-invariance of the path integral measure under chiral (γ_5) rotations. Topological properties of the QCD vacuum!

K. Fujikawa, PRL. 42, 1195 (1979)

$$\partial^\mu J^5_\mu(x) = \frac{n_f \alpha_s}{2\pi}\ \mathrm{Tr}\left(F_{\mu\nu}(x)\tilde{F}^{\mu\nu}(x)\right)$$

topological charge density

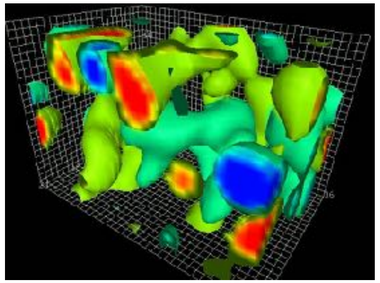

D. Leinweber

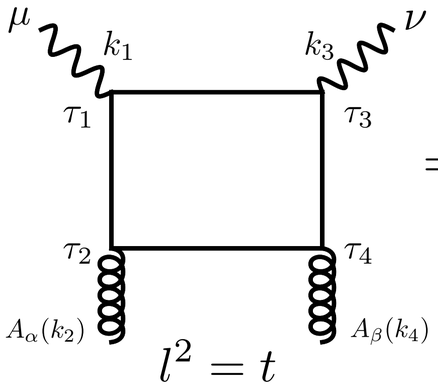

infrared anomaly pole

twist-4 GPD $\tilde{\mathcal{F}}(x,\xi,t)$

$$= \sum_f e_f^2 \frac{\alpha_s}{i\pi M_N} \frac{l^\mu}{l^2} \int_{x_B}^1 \frac{dx}{x}\left(1 - \frac{x_B}{x}\right) \int \frac{d\xi}{2\pi} e^{-i\xi x} \langle P', S|\mathrm{Tr_c} F_{\alpha\beta}(\xi n)\tilde{F}^{\alpha\beta}(0)|P,S\rangle + \text{non-pole terms}$$

Tarasov, Venugopalan, 2020; Bhattacharya, Hatta, Vogelsang, 2023
Bhattacharya, Hatta, Schoenleber, 2024

The resolution of the anomaly pole is deeply related to the famous $U_A(1)$ problem in QCD: instead of an infrared pole $1/l^2$ of a "primordial" ninth Goldstone boson $\bar{\eta}$ there is a heavy η' ($m_{\eta'} \approx 957 MeV$)

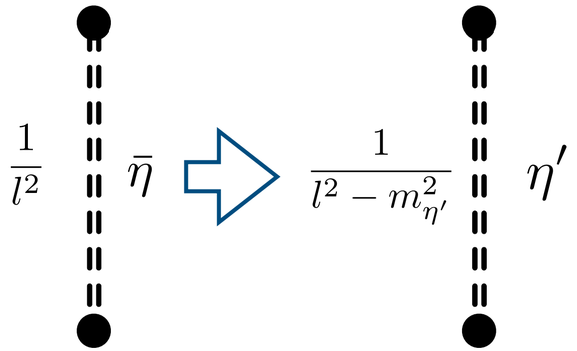

- Anomalies constraint GPDs
- Non-perturbative relations between GPDs mediated by anomalies ($\tilde{E}$ and $\tilde{\mathcal{F}}$)
- Similar for the DIS structure functions ($t \to 0$)

$$\Delta\Sigma|_{m=0} = \frac{N_f}{M_N}\sqrt{\chi'_{\mathrm{QCD}}(0)}\, g_{\bar{\eta}NN}$$

Shore, Veneziano, 1992; Tarasov, Venugopalan, 2025

QCD energy-momentum tensor

Relation to the QCD energy-momentum tensor (EMT) is a unique feature of GPDs

$$T^{\mu\nu} = \bar{\psi}\gamma^{\mu}\frac{i}{2}\overleftrightarrow{D}^{\nu}\psi - G^{a\mu\lambda}G^{a\nu}{}_{\lambda} + \frac{1}{4}g^{\mu\nu}G^2$$

$$p_{q,g}(r) = \frac{1}{6Mr^2}\frac{d}{dr}r^2\frac{d}{dr}D_{q,g}(r) - M\bar{C}_{q,g}(r)$$

pressure inside proton

Mass and pressure

EMT provides access to the mechanical properties of the proton:

$$\langle p'|T^{\mu\nu}_{q,g}|p\rangle = \bar{u}(p')\left[A_{q,g}(t)\gamma^{(\mu}P^{\nu)} + B_{q,g}(t)\frac{P^{(\mu}i\sigma^{\nu)\alpha}\Delta_{\alpha}}{2M} + D_{q,g}(t)\frac{\Delta^{\mu}\Delta^{\nu} - g^{\mu\nu}\Delta^2}{4M} + \bar{C}_{q,g}(t)Mg^{\mu\nu}\right]u(p)$$

$$J_{q,g} = \frac{1}{2}(A_{q,g} + B_{q,g})$$

Total angular momentum

GFFs A_a, B_a, D_a can be related to leading twist GPDs and probed at EIC:

$$\int dx x H_q(x,\xi,t) = A_q(t) + \xi^2 D_q(t)$$

$$\int dx x E_q(x,\xi,t) = B_q(t) - \xi^2 D_q(t)$$

D_{u+d} can be extracted from CFF

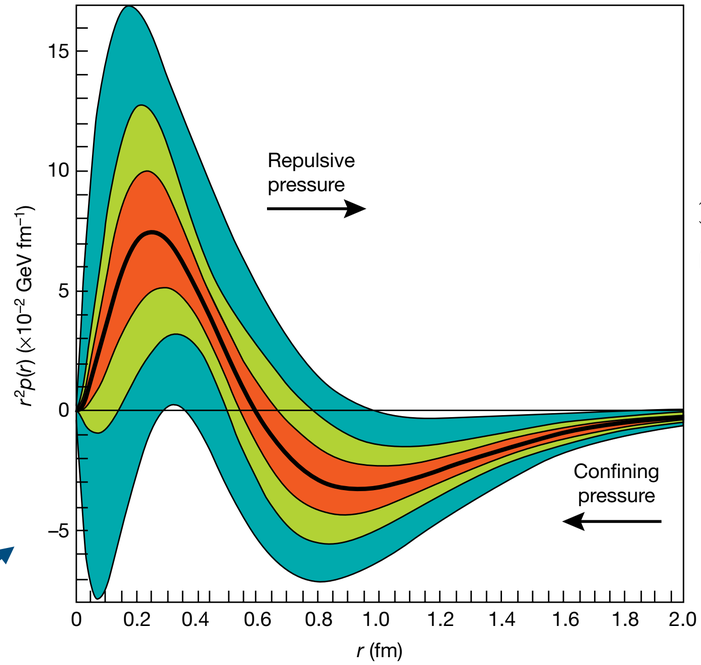

Burkert, Elouadrhiri, Girod, 2018

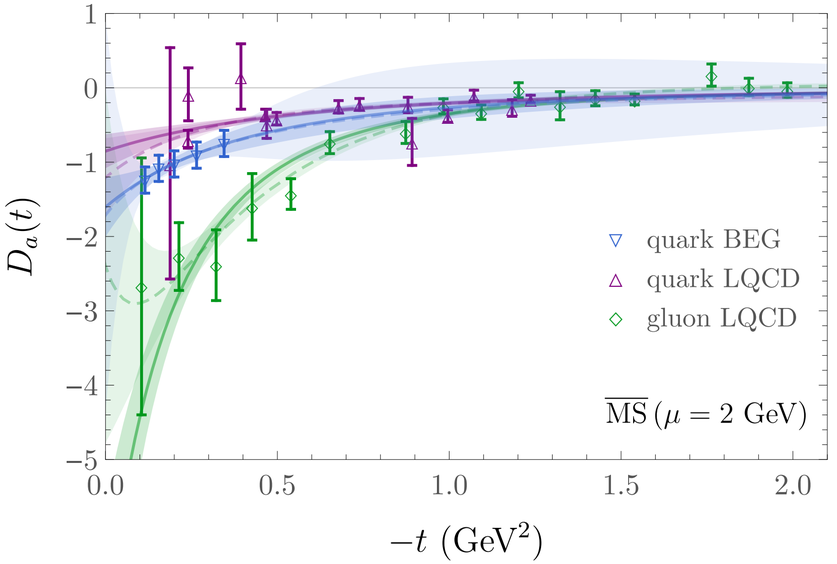

Shanahan, Detmold, 2018

How does the mass of the nucleon arise?

Trace of EMT:

$$T^{\mu}_{\mu} = (T_q)^{\mu}_{\mu} + (T_g)^{\mu}_{\mu} = \frac{\beta(g)}{2g} F^{\mu\nu,a} F^{a}_{\mu\nu} + \sum_q m_q (1+\gamma_m) \bar{\psi}_q \psi_q$$

trace anomaly — chiral symmetry breaking

matrix element: $\langle P|(T_{q,g})^{\mu}_{\mu}|P\rangle = 2M^2(A_{q,g} + 4\bar{C}_{q,g})$

Mass of the nucleon can be extracted from the trace of EMT:

$$\langle P|T^{\mu}_{\mu}(0)|P\rangle = 2P^2 = 2M_n^2 \quad \Rightarrow \quad M_n = \sum_{f=q,g} \frac{\langle P|T_f^{00}(0)|P\rangle}{2P^0}$$

nucleon's rest frame

- Can be further decomposed into gauge invariant terms
- Each term has its own physical interpretation and relation to observables
- But the decomposition is not unique, different schemes are available
- Trace anomaly can be extracted directly from near-threshold quarkonium production

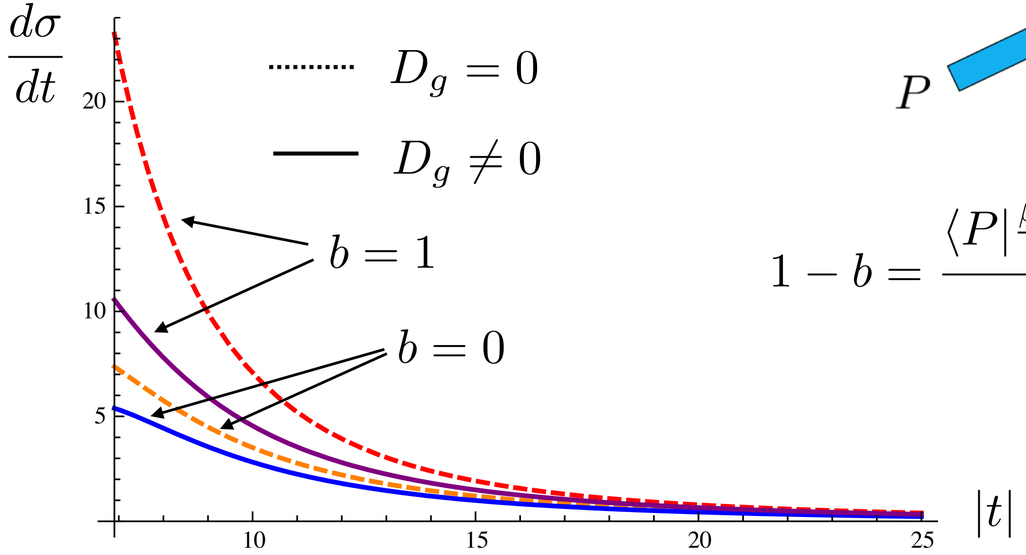

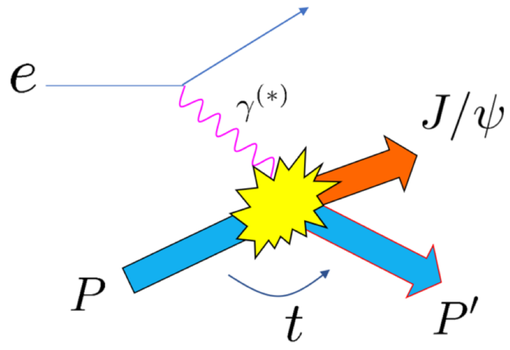

$$1 - b = \frac{\langle P|\frac{\beta(g)}{2g} F^2|P\rangle}{2M_N^2}$$

Jets at EIC

Became an active area of research. EIC is a relatively low energy machine → smaller multiplicities and $p_\perp$, but there are certain advantages, e.g. less underlying events, clean environment to study jets

Jets provide more direct access to underlying partonic subprocesses:

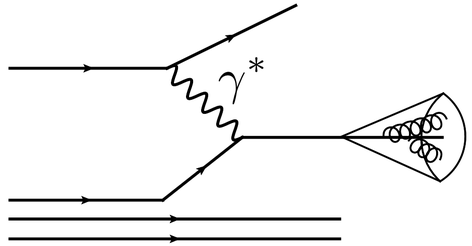

single jet

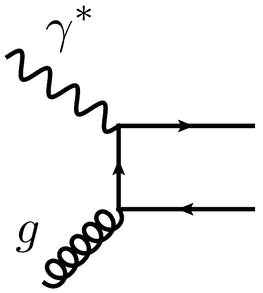

dijet

In many aspects the research program of jets at EIC is similar to studies of jets in pA collisions:

jets in cold nuclear matter, insights into hadronization, jet modification in eA

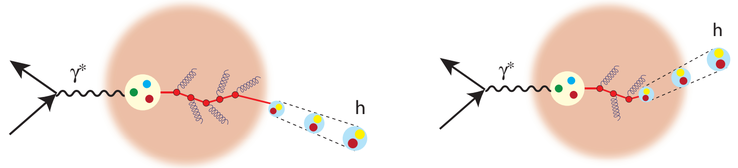

jet production in ep collisions

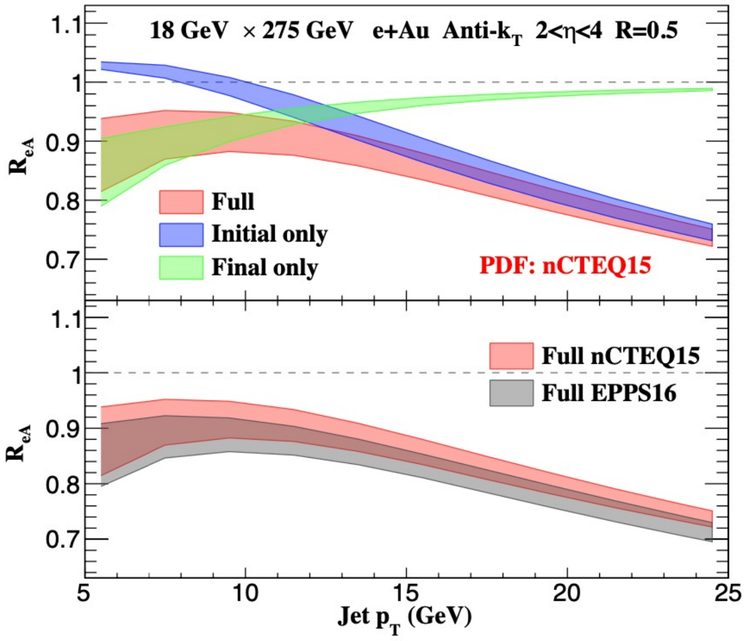

Kang, Ringer, Vitev, 2017; Li, Vitev, 2020;

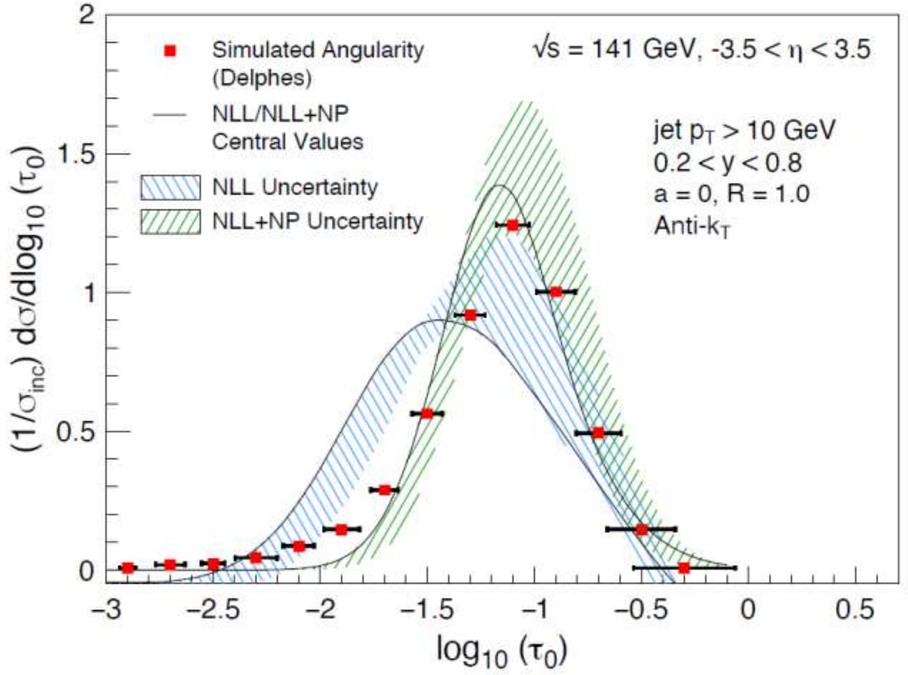

jet substructure

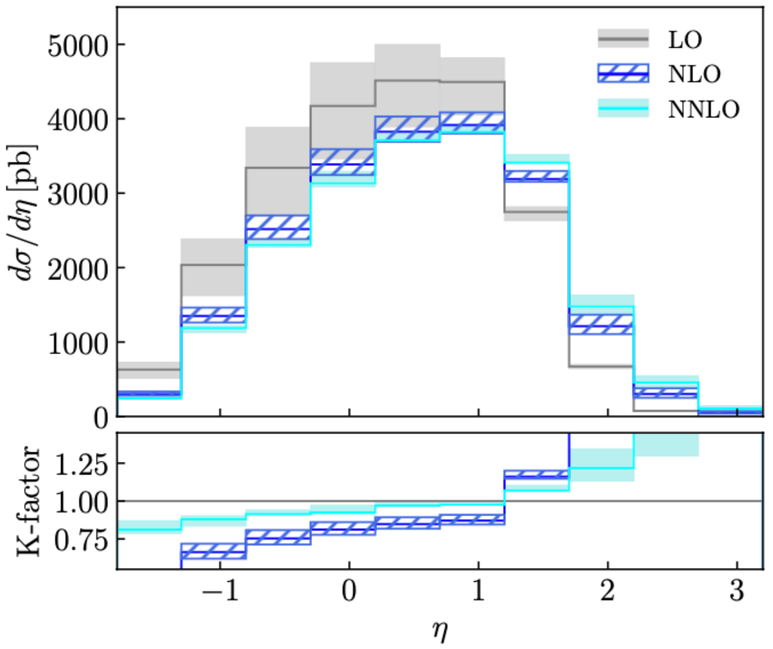

Aschenauer, Lee, Page, Ringer, 2020

Borsa, de Florian, Pedron, 2020

Jets at EIC: interplay with other fields

Many studies of jets at EIC will be complimentary to other components of the program, but also unique on its own

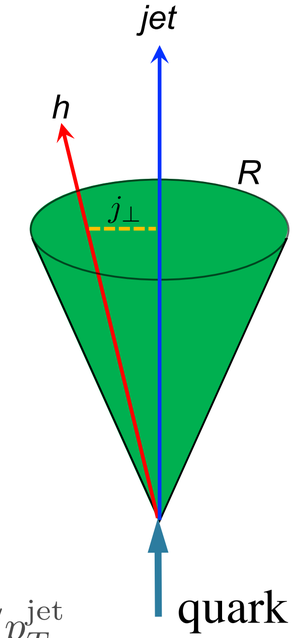

$z_h = p_T^{\rm h}/p_T^{\rm jet}$

$j_\perp$: hadron transverse momentum with respect to the jet

Jet measurements for 3D imaging: hadrons in jets provide access to TMDPDFs and TMDFFs

Kang, Lee, Shao, Zhao, 2021

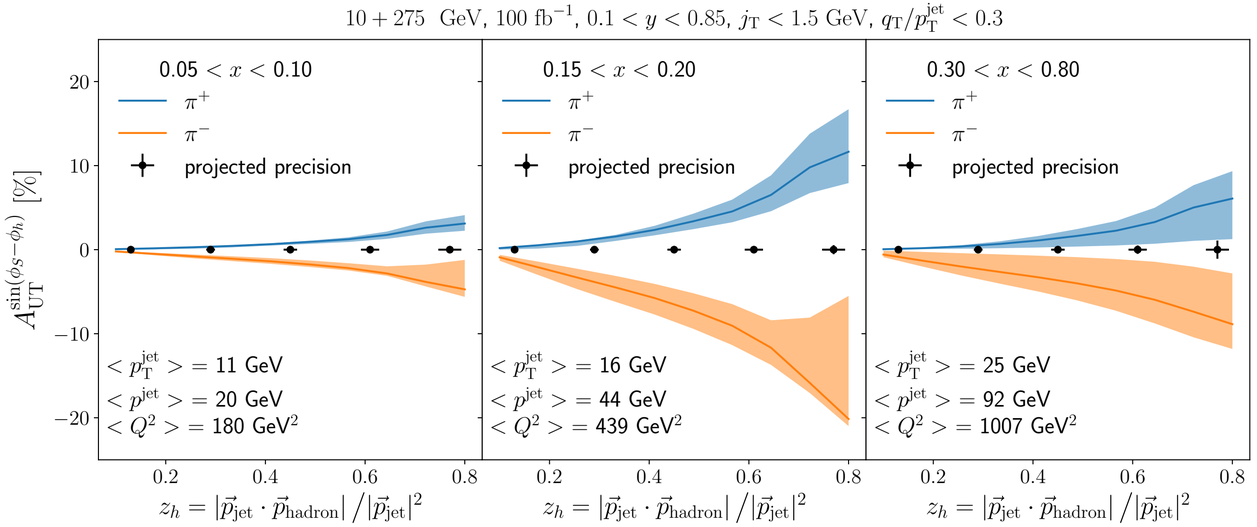

Event shape observables like energy-energy correlator (EEC) or transverse-energy-energy correlator (TEEC) are sensitive to TMDPDFs in the back-to back limit

$$\mathbf{TEEC} = \sum_h \int \mathrm{d}\sigma_{\rm DIS} \frac{E_{T,h}}{\sum_i E_{T,i}} \delta\left(\tau - \frac{1+\cos\phi}{2}\right)$$

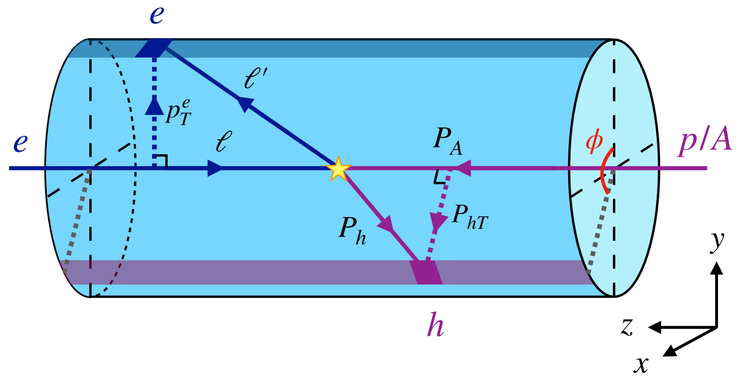

Li, Vitev, Zhu, 2020
Li, Makris, Vitev, 2021
Kang, Penttala, Zhao, Zhou, 2023

$$\mathbf{TEEC} \equiv \frac{\mathrm{d}\sigma}{\mathrm{d}\tau\,\mathrm{d}y_e\,\mathrm{d}^2\boldsymbol{p}_T^e} = \sigma_0 H(Q,\mu) \sum_q e_q^2 \frac{p_T^e}{\sqrt{\tau}} \int_0^\infty \frac{\mathrm{d}b}{\pi} \cos\left(2b\sqrt{\tau}p_T^e\right) f_q^{(u)}\left(x,b,\mu,\zeta/\nu^2\right) S_{nn_h}(b,\mu,\nu) J_q^{(u)}(b,\mu,\zeta'/\nu^2)$$

Thank you for your attention!